PERFORMANCE ASSESSMENT OF VAPOR COMPRESSION SYSTEMS UTILIZING LOW GLOBAL WARMING POTENTIAL HYDROCARBONS AND CARBON DIOXIDE AS WORKING FLUIDS

A Thesis Presented

By

Bassam S Aljohani

to

The Department of Mechanical and Industrial Engineering

In partial fulfillment of the requirements
for the degree of

Master of Science

in the field of

Mechanical Engineering

Northeastern University
Boston, Massachusetts

August 2018

ABSTRACT

The air conditioning (AC) refrigerants such as chlorofluorocarbons (CFC) as well as hydrofluorocarbons (HFC) have been major factor affecting on the global warming. These harmful refrigerants have long life-span emissions and can travel to the stratospheric layer (20-50 km above the earth's surface) that possess detrimental ultraviolet (UV) radiation and through a reactive chain a chlorine atom forms that break this beneficial layer of the ozone. The drawbacks of breaking this layer are countless, but to name one the (UV) radiation causes death to many species because of its high ozone depletion potentials (ODP) and high global warming potentials (GWP). Alternative substitutes to these refrigerants are the universally accepted demands of using low global warming potentials (low GWP) and low ozone depletion potentials (low ODP) refrigerants such as carbon dioxide and hydrocarbons (HC). In this thesis, a mixture of carbon dioxide (CO_2) with hydrocarbons (HC) such as propane (C_3H_8), propylene (C_3H_6), n-butane (C_4H_{10}), and dimethyl ether (C_2H_6O) are implemented to substitute the current refrigerants. The high-pressure problematic associated with carbon dioxide is reduced upon mixing with hydrocarbons (HC). In addition, the blending process lowers the flammability characteristic of the hydrocarbons (HC) since carbon dioxide is non-flammable refrigerant. The implementation was made based on the refrigerants' thermodynamic characteristics, low toxicity, low global warming potentials (GWP), and zero ozone-depletion potentials (ODP). The study was performed on simulations by MATLAB code linked with REFPROP database for vapor compression cycle system consisting of compressor, condenser, throttling valve, energy exchanger, and evaporator. The blend of these hydrocarbons with carbon dioxide enhances the performance of the system at mole fraction of 10% and 90% of carbon dioxide. The blend of propane as well as propylene with carbon dioxide at these ratios reached the highest coefficient of performance (COP). Whereas the blend of n-butane with carbon dioxide has decreased the coefficient of performance (COP). The dimethyl ether with carbon dioxide has resulted in an intermediate coefficient of performance (COP) between the other two hydrocarbons. The volumetric cooling capacity (Qc) has been enhancing with the addition of carbon dioxide (CO_2) to maximum at mole fraction of 100% carbon dioxide (CO_2).

ACKNOWLEDGMENT

I would like to express the deepest appreciation to my committee chair Professor Hameed Metghalchi for his guidance and support. Without your assistance and guidance, I wouldn't be where I am today

I would like to extend my appreciation to Professor Yiannis Levendis who provided insight and expertise that greatly assisted this research. Without your advice and expertise, I wouldn't achieve to this point.

Last but not least, I would like to further send many thanks to the laboratory team for all the effort put into this research; Khalid S. Aljohani, Ziyu Wang, and Yelishala Chandra Sai.

Dedicated to my parents Saad and Affaf for offering me the opportunity to attend Northeastern University and also for always being supporting and motivating me.

Dedicated to my wife Dhuha for her patient and motivational words when I need them throughout this journey, I could not have done it without you.

TABLE OF CONTENTS

LIST OF TABLES

LIST OF FIGURES

Nomenclature

c_p	Specific heat at constant pressure (KJ/Kg-K)	ρ_0	ideal gas density (Kg/m^3)
c_v	Specific heat at constant volume (KJ/Kg-K)	c_p^0	ideal gas heat capacity (KJ/Kg-K)
ρ_c	Critical density (mol·dm^{-3}) (Kg/m^3)	$\overline{x}$	molar composition
T_c	Critical temperature (K)	δ_m	reduced mixture density (Kg/m^3)
T_{tp}	Triple point temperature (K)	τ_m	inverse reduced mixture temperature (K)
P_c	Critical Pressure (MPa)	$\Delta\alpha^r$	departure function.
S_u	Laminar burning speed (cm/s)	Z	compressibility factor
P_{tp}	Triple point pressure (Pa)	p	conventional pressure (Pa)
a	Helmholtz energy (KJ)	h	conventional enthalpy (KJ)
α	dimensionless Helmholtz energy	T	conventional temperature (K)
h^0	ideal gas enthalpy (KJ)	s	conventional entropy (J·mol^{-1}·K^{-1})
TG	Temperature Glide	u	internal energy (KJ)
s^0	ideal gas entropy (J·mol^{-1}·K^{-1})	Δh_c	Heat of combustion (MJ/Kg)
T_{nbp}	Normal boiling temperature (K)	T_a	Ambient temperature (K)
T_E	Environment temperature (K)	LFL	Lower flammable limit (% vol)
UFL	Upper flammable limit (% vol)	T_{ig}	Ignition Temperature (K)
T_{bp}	Boiling point (K)	T_{dp}	Dew point (K)

Abbreviations

REFPROP	Reference Fluid Thermodynamic and Transport Properties
NIST	National Institute of standards and Technology
EOS	Equation of State
M.W.B.R.E.	Modified Benedict Webb Rubin Equation of State
GERG	Groupe Européen de Recherche's Gazières
COP	Coefficient of Performance
GWP	Global Warming Potential
ODP	Ozone Depletion Potential
ASHRAE	American Society of Heating, Refrigerating, and Air-Conditioning Engineers

1. Introduction

The National Oceanic and Atmospheric Administration has studied the effects of the global climate temperature and the sea level. They concluded that there is an increase in the temperature of the globe as well as the sea level has risen due to the greenhouse effect generated by harmful gases [1]. Harmful gases such as the refrigerants used in air conditioning systems, namely chlorofluorocarbons (CFC) in which its long life-span emissions can travel to the stratospheric layer (20-50 km above the earth's surface) that possess detrimental ultraviolet radiation and through a reactive chain a chlorine atom forms that break this beneficial layer of the ozone. The drawbacks of breaking this layer are countless, but to name one the UV radiation causes death to many species because of its high ozone depletion potentials (ODP) [2]. Eventually, the hydrofluorocarbons (HFC) have replaced the CFC refrigerants, however the HFC has also impacted on the global climate due to its high global warming potentials (GWP) [2]. As such, mandated acts have to be considered. Phase-out decision of HFC has been agreed in Protocols meetings worldwide [3]. Alternative refrigerants must replace the existing ones with fewer environmentally concerns such as low global warming potentials (GWP), low ozone-depletion potentials (ODP), low toxicity, and adequate air conditioning (AC) characteristics. The alternative refrigerants can be pure substance, like carbon dioxide (CO_2) or a blend of refrigerants such as hydrocarbons (HC) mixed with a mole fraction of carbon dioxide (CO_2). In this work, a mixture of carbon dioxide (CO_2) and hydrocarbons (HC) such as propane, propylene, n-butane, and dimethyl ether are suggested to replace the existing refrigerants. The suggestion was made based on their adequate thermodynamics characteristics, low toxicity, low global warming potentials (GWP), and zero ozone-depletion potentials (ODP). The issue of high pressure of carbon dioxide (CO_2) is reduced upon mixing with hydrocarbons (HC). The flammability of hydrocarbons (HC) is the main problematic in which it is blended with Carbon dioxide to reduce their flammability.

1.1 Propane

Propane (C_3H_8) is alkane-group gas found at atmospheric conditions and usually compressed to liquid for transportation purposes between refineries and commercials. This gas is termed as liquefied petroleum gas (LPG) for convenience and has excellent thermodynamics properties and moderate volumetric capacity of refrigeration as compared to the widely used R-410a and R-134a. Also, propane is a natural refrigerant and investigated in respond to the Kyoto Protocol agreement to reproduce natural refrigerants such as Ammonia and carbon dioxide utilized in air conditioning systems.

1.2 Propylene

A small fraction of propylene (C_3H_6) and n-butane (C_4H_{10}) is also termed in the (LPG). Propylene is propane with fewer hydrogen atoms and has become a future substitute of (HFC) in the 1990s. It has (ODP = 0), low (GWP $\leq$2), non-toxicity, and suitable for low and medium temperature refrigeration systems.

1.3 n-Butane

n-Butane (C_4H_{10}) is not widely used as refrigerants and it has a good thermodynamics characteristic. The (COP) of refrigeration is much higher than the used R-134a but its flammability characteristic limits its use in the automotive industries. The (COP) of n-butane is also higher than the isobutene for reverse Rankin cycle. Its high critical temperature makes it operate on medium and high temperature conditions with excellent thermodynamics properties. It has (ODP = 0), low (GWP $\leq$3), and non-toxicity.

1.4 Dimethyl ether

Dimethyl ether is (C_2H_6O) is oxygenated-HC and has the potential to replace many (HFCs) such as R-12 and R-502 due to its saturated temperature and pressure relationship close to that of R-12. It has good heat transfer characteristics, (ODP = 0), very low (GWP $\leq$0.002), and non-toxicity characteristic. The flammability of the dimethyl ether is the main reason to it is delayed applications in the air conditioning systems.

1.5 Carbon Dioxide

Carbon dioxide (CO_2) is a natural refrigerant used extensively in many recent applications. It has the highest volumetric capacity among all hydrocarbons and (ODP = 0) as well as (GWP of $=1$) by definition. Additionally, pure carbon dioxide (CO_2) has non-flammability characteristic in which it makes it a perfect blend with hydrocarbons. The sole drawback of the carbon dioxide its high critical pressure and low critical temperature characteristics that force the thermodynamics cycle to operate on transcritical cycle in hot-climate applications. Details on the transcritical cycle drawbacks are discussed later in this report.

1.6 Blend of Carbon Dioxide (CO_2) and Hydrocarbons (HC)

Blend of carbon dioxide (CO_2) and hydrocarbons (HC) is the scope of this thesis operating on unitary refrigeration systems. The carbon dioxide (CO_2) is used due to its high volumetric capacity and non-flammability characteristics to enhance the refrigeration capacity as well as to reduce the flammability associated with hydrocarbons (HC). As a result, ensuring that the system has safety measures considered as part of the research and therefore can be considered in real world applications of air conditioning (AC) systems. This safety measures have not been conducted in the literature and therefore their work is not applicable in real world cases. In this study, critical considerations on the peak pressure rise of the carbon dioxide (CO_2) and its effects of transcritical cycle are discussed. In addition, extreme cases for refrigeration system for both the refrigerator and fridge in hot climate room temperature are also studied.

2. Equations of State and the Thermophysical Properties

Thermo-physical properties are defined as the properties of a fluid or a multi-fluid mixture, that vary with change in temperature or pressure or composition of the mixture. The thermo-physical properties can be derived using equation of state (EOS). Where EOS is defined as a thermodynamic equation which relates variables like pressure, temperature, volume and internal energy, defining a known state of a substance. A widely used example of EOS is the ideal gas law (PV = nRT). For determining these thermophysical properties we have used a software program called REFPROP 9.1 [4] by NIST. A detailed explanation of how to use this program and its limitations are given in the REFPROP 9.1 user manual [5].

The REFPROP code is used to solve the EOS for a given fluid/mixture. REFPROP code was chosen because of its widespread use in industrial applications, as well as its use in several thermodynamic textbooks and research papers. To solve the EOS at any state, we need to input two parameters to define the state of a fluid, such as pressure and temperature. After defining a state, the code calculates the thermophysical properties of a fluid at that state. Saturated states for liquid-vapor equilibrium can also be calculated using a single state point as an input. The T-s and P-V diagrams can also be obtained. Details on the equation of state used by REFPROP are given in ensuing sections of this thesis, along with the validation of the properties derived from the REFPROP EOS by comparing its output with a specific EOS, that of the modified Webb-Benedict-Rubin equation (MWBR) in tabular form [11]. The EOSs used in REFPROP for hydrocarbons and carbon dioxide are expressed in the form of Helmholtz free energy with independent variables of density and temperature, and in the case of mixtures the molar composition of the participating fluids. This Helmholtz energy EOS serves as a base for determining the thermo-physical properties of a fluid with the aid of differential equations.

For different fluids/mixtures the EOSs used by REFPROP have different coefficients and parameters, that are derived mainly by fitting available experimental data for those fluids to the EOS. For illustration purposes, the EOS for propane (C3H8) is exemplified herein. The EOS for other hydrocarbons has similar approach to that for propane. EOS, hence the propane EOS is representative for all hydrocarbons in this report. The EOS for carbon dioxide has also been exemplified, along with the EOS for multi-fluid mixtures.

These equations of state (EOS) serve as a base for determination of thermodynamics properties with the aid of partial differential equation (PDE). It is critically important to have an accurate equation of state (EOS) since all thermodynamics properties are determined using such (EOS). The (EOS) will serve as a reference for calculating enthalpies at different state points. Determining accurate results pertaining enthalpy is crucial since the analysis will be analyzed according to each state point using the equation of state. This thesis studies two equations of states that are widely used to determine the enthalpy of pure substance, specifically propane. The equation of state is of National Institute of Standards and Technology (NIST), namely equation of state using Helmholtz free energy function by Lemmon and Mclinden [7].

3. REFPROP-NIST and the M. B.W. R. Equations of States

The purpose of choosing (a) the (REFPROP-NIST) equations of state is because of their high level of accuracy, and (b) the (MBRW) equation of state is because of its use in several thermodynamics books. The NIST equations of state are expressed in the form of Helmholtz free energy with independent variables of density and temperature (in addition of the molar composition ($\overline{x}$) for multi-component fluids). The NIST equation of state is written in term of Helmholtz free energy and thermodynamics properties at different states can be obtained by differentiation of this equation. Other equations of state used prior to 2008 are by Sychev et al. in (1991) in terms of the compressibility factor with 50 terms and has no exponential part. In 1982, Goodwin and Haynes developed equation of state used a unique functional form that cannot be implemented in computational algorithms [7]. In this thesis, Two EOSs are intensively tested and validated for a certain range of temperature and pressure as well as in term of mole fraction in the case of mixtures.

4. Equation of State of Propane

The EOS used to calculate the thermodynamic properties of propane is developed by Eric W. Lemmon and Mark O. McLinden [7] which is valid for temperatures ranging from the triple point temperature of propane of 82.525 to 650 K and for pressures up to 1000 MPa. The important physical constants and characteristics of propane apart from critical point and triple point used in the derivation of the Helmholtz energy-based EOS are shown in Table 1. A change of initial temperature and pressure is introduced on Table 1. Corresponding properties for other hydrocarbon-based refrigerants of interest to this study are given in Table 2. This table is adoption for the purpose of comparison between two equations of states [7].

Table 1: Physical constants and characteristic properties of propane.

Symbol	Description	Value
T_c	Critical temperature	369.89 K
P_c	Critical pressure	4.2512 MPa
ρ_c	Critical density	5 mol/dm^3
T_{tp}	Triple point temperature	85.525 K
P_{tp}	Triple point pressure	0.00017 Pa
ρ_{tpv}	Vapor density at the triple point	2.4·10-10 mol / dm^3
ρ_{tpl}	Liquid density at the triple point	16.626 mol / dm^3
T_{nbp}	Normal boiling point temperature	231.036 K
ρ_{nbpv}	Vapor density at the normal boiling point	0.0548 mol / dm^3
ρ_{nbpl}	Liquid density at the normal boiling point	13.173 mol / dm^3
To	Reference temperature for ideal gas properties	298.15 K
Po	Reference pressure for ideal gas properties	0.101352 MPa

Table 2: Thermophysical constants of other hydrocarbons.

Refrigerants	Critical Temperature (K)	Critical Pressure (kPa)	Critical Density (kg/m^3)	Normal Boiling Point (K)	Molar mass (kg/kmol)
propane [7]	370	4251	220	231	44
dimethyl ether [15]	400	5337	274	248	46
n-butane [16]	425	3796	228	273	58
R-1234yf [16]	368	3382	475	244	114
carbon dioxide [10]	304	7377	468	195	44

4.1 Critical Point

The critical point defines the state of the substance or mixture at liquid state, vapor state, or at super critical states. It is important to obtain the critical point of a substance or a mixture when developing an equation of state due to it is highly acts as a reducing parameter on the equation of state [7]. At the critical point, a substance or a mixture is existed in single phase and has reached to it is endpoint of equilibrium. Above the critical point, the substance or mixture will behave differently, namely the un-defined region of supercritical zone. Figure 1 shows the critical temperature variations with respect to the addition of carbon dioxide mole fraction. Several studies have illustrated the critical temperature, density, and pressure within 5 percent variations [7]. Among these studies, the critical temperature, density, and pressure have been selected based on propane by Lemmon and Mclinden [7] as follows:

For propane (C_3H_8)

$$T_c = (369.89 \pm 0.03)\ K$$
$$\rho_c = (5.00 \pm 0.04)\ mol / dm^3$$
$$P_c = (4.2512 \pm 0.005)\ MPa$$

For carbon dioxide (CO_2)

$$T_c = (304.128 \pm 0.015)\ K$$
$$\rho_C = (467.60 \pm 0.6)\ kJ/m^3$$
$$P_c = (7.3773 \pm 0.003)\ MPa.$$

4.2 Critical Temperature Changes with Mole Fractions of Carbon Dioxide

The promising refrigerants of hydrocarbons (HC) and hydro fluorine olefin (HFO) tend to have higher critical temperatures than the carbon dioxide (CO_2). Mixing these refrigerants with carbon dioxide will lower their critical temperatures due to the low critical temperature of (CO_2). According to Figure 1, the n-butane, dimethyl ether, R-1234ze (E), and R-1234yf have slightly higher critical temperatures upon mixing with (CO_2) comparing to the other two refrigerants, in which it makes them a potential blend in cold-climates. For this reason, these refrigerants can operate at subcritical cycle up to 85 % of (CO_2) mixture (mole fraction) in such climates. Propane and propylene have a lower critical value of temperatures than those previously mentioned refrigerants and as a result, they operate at both the subcritical and transcritical cycles upon mixing with (CO_2).

Table 3: Critical temperature as a function of mole fraction of carbon dioxide.

Mixture	propane	n-butane	dimethyl ether	propylene	R1234yf	R1234ze(E)
x (CO_2)	Tcr (K)	Tcr (K)	Tcr (K)	Tcr (K)	Tcr (K)	Tcr (K)
0	369	425	400	364	368	383
0.1	366	418	397	362	370	382
0.2	361	411	392	358	370	379
0.3	355	404	386	354	369	375
0.4	346	394	379	348	366	371
0.5	337	383	372	342	361	365
0.6	328	368	362	335	354	357
0.7	318	352	351	327	345	348
0.8	310	335	339	319	333	337
0.9	305	318	323	312	320	323
1	304	304	304	304	304	304

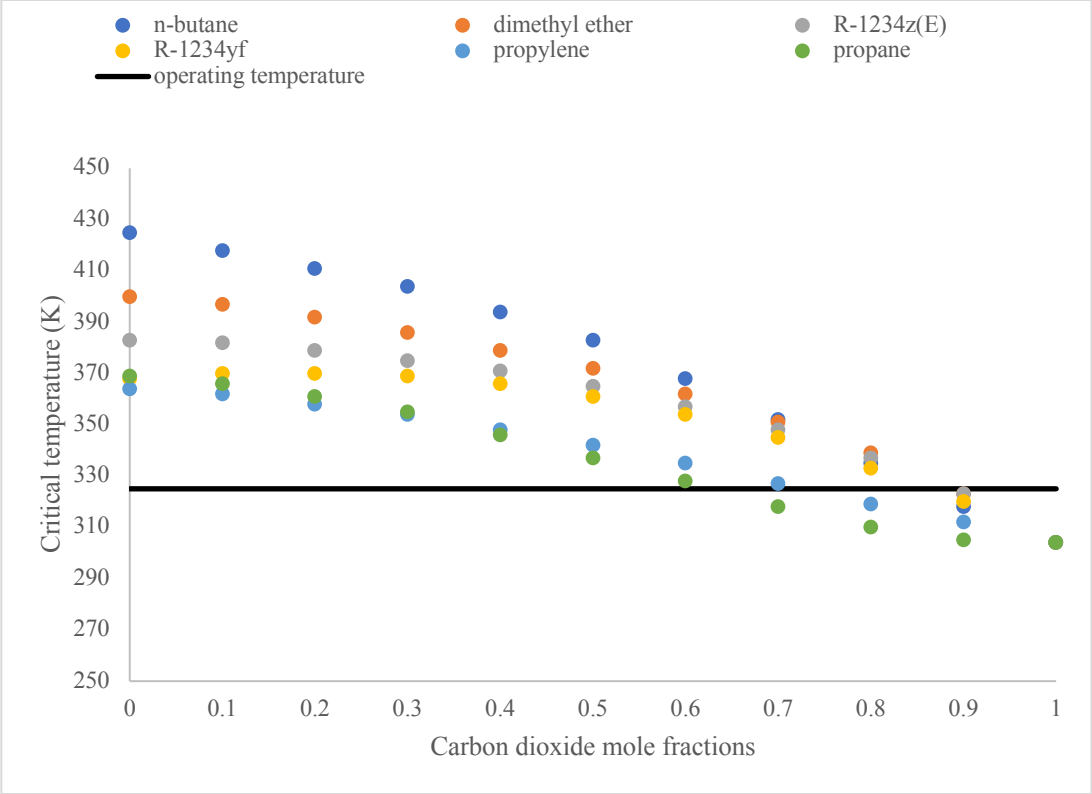

Figure 1: Critical temperatures as a function of carbon dioxide mole fraction of potential refrigerant.

4.3 Critical Pressure Changes with Mole Fractions of Carbon Dioxide

The critical pressures of the hydrocarbons (HC) and hydro fluorine olefin (HFO) increase as the carbon dioxide (CO_2) mole fraction increases. This increase is mainly due to the higher critical pressure of the (CO_2). According to Figure 3, dimethyl ether has the highest critical pressure followed by propylene, propane, n-butane, R-1234ze (E), and R-1234yf respectively. A dome and a drop are noticed upon mixing with mole fraction of (50 to 90 %) of carbon dioxide (CO_2) which is due to the artifact of the binary mixture. It can be seen that the hydrocarbons (HC) have higher critical pressures while the R-1234ze (E) and R-1234yf have relatively lower critical pressures in which it makes them a future blend for systems that require lower operating pressures, specifically up to (50 % ofCO_2).

Table 4: Critical pressure as a function of mole fraction of carbon dioxide.

Mixture	propane	n-butane	dimethyl ether	propylene	R1234yf	R1234ze (E)
x (CO_2)	Pcr (kPa)	Pcr (kPa)	Pcr (kPa)	Pcr (kPa)	Pcr (kPa)	Pcr (kPa)
0	4212	3796	5336	4555	3382	3634
0.1	4959	4471	5936	5245	4088	4266
0.2	5574	5191	6513	5822	4771	4870
0.3	6121	5991	7074	6359	5475	5486
0.4	6560	6841	7611	6849	6185	6112
0.5	6818	7572	8096	7269	6864	6727
0.6	6872	8078	8511	7585	7460	7317
0.7	6807	8238	8775	7762	7903	7823
0.8	6764	8068	8796	7779	8137	8163
0.9	6909	7719	8441	7655	8063	8164
1	7377	7377	7377	7377	7377	7377

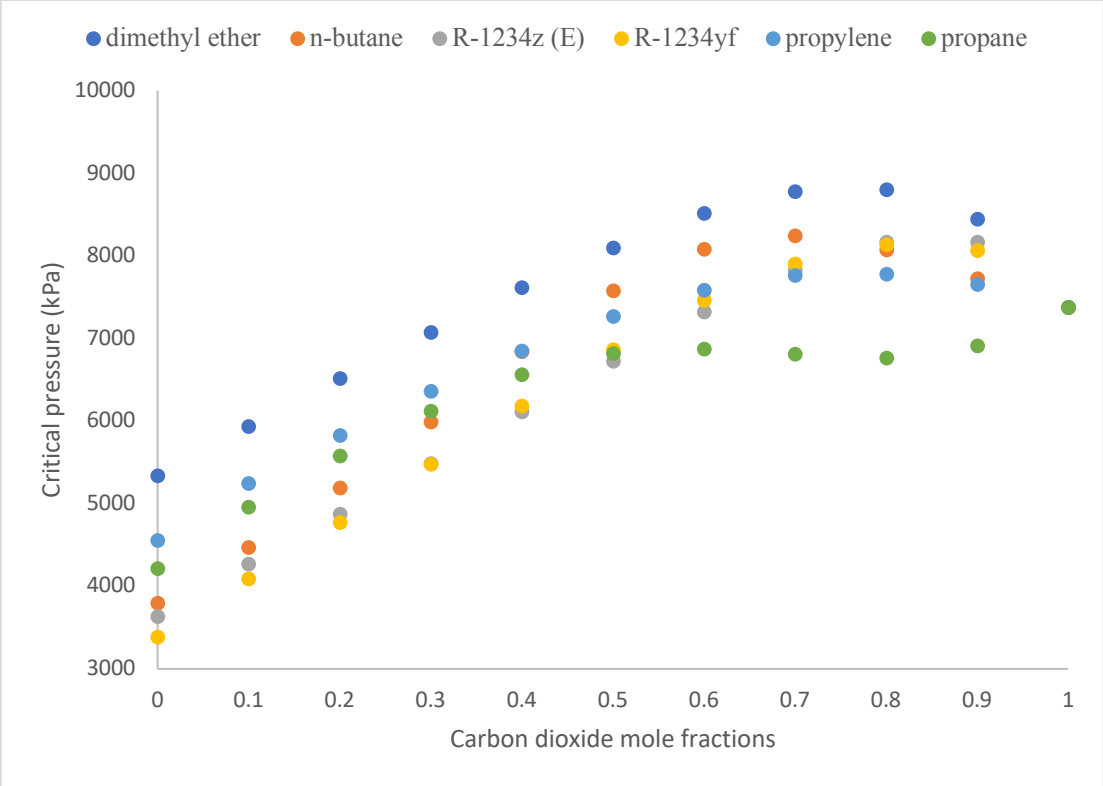

Figure 2: Critical pressures as a function of carbon dioxide mole fraction of potential refrigerant.

4.4 Triple Point

It is worthwhile to note that the triple point is defined as the state point where all three phases coexist (liquid, gas, and solid). For propane, the triple temperature(T_{tp}) is determined by Perkin et al. [8] and the triple pressure is based on Perkins et al. was measured at (P_{tp}) and shown in Table 1. In addition, Table 5 shows the important parameters of carbon dioxide.

Table 5: Characteristics properties and constant of carbon dioxide.

Symbol	Description	Value
R	Molar gas constant	8.314 472 J/mol·K
M	Molar mass	44.0098 g / mol
T_c	Critical temperature	304.128 ± 0.015 K
P_c	Critical pressure	4.2512 MPa
ρ_c	Critical density	467.60 kJ/m^3
T_{tp}	Triple point temperature	216.003 K
P_{tp}	Triple point pressure	0.51795 MPa
T_o	Reference temperature for ideal gas properties	298.15 K
P_o	Reference pressure for ideal gas properties	0.101325 MPa
h_0^0	Reference ideal gas enthalpy at T_o	0 J/mol
s_0^0	reference ideal gas entropy at T_o and P_o	0 J/mol ·K

4.5 Subcritical and Transcritical Cycles

The operating cycles for the specified operating temperature condition (325.15 K, 52 ℃) are on the subcritical and transcritical cycles. This temperature is only an example to illustrate the subcritical and transcritical point of view. There are different considered temperatures ranging from – 15 to 25 ℃ that have been considred to suite the application of the air conditioning systems. According to Figure 1, the addition of (CO_2) mole fraction to both hydrocarbons (HC) and hydrofluorineolefin (HFO) will result in operating at the subcritical and transcritical cycle due to the high-pressure rejection of (CO_2). In addition, the n-butane, dimethyl ether, R-1234ze (E), and R-1234yf will operate at the subcritical cycle up to approximately 85 % of (CO_2) mole fraction. Higher mole fractions ($\geq$ 85 % of CO_2) imply that the system will operate above the saturated liquid-vapor dome, namely the supercritical region (transcritical cycle). In the operating mode of supercritical region, the system requires a careful design with highly-temperature resistive materials that operate at the supercritical region. In the case of propane and propylene with addition of (CO_2) mole fraction, the system operates on the supercritical region at the present of ($\geq$ 65 % CO_2). The (CO_2) operates on the transcritical cycle only for the specified operating temperature. At room temperature of 25 ℃ degress, the operating cycle for these hydrocarbons are subcritical that is because condenser exit temperature is well below their critical temperatures.

4.6 Functional form of the Equation of State for Propane

Equation of State in terms of Helmholtz free energy by Lemmon and Mclinden [7]:

$$a(\rho, T) = a^0(\rho, T) + a^r(\rho, T) \quad (1)$$

Where a = Helmholtz energy, a^0 = ideal gas contribution, a^r = residual Helmholtz energy which corresponds to the influence of intermolecular forces. This functional form of Equation of State is applied for propane and propylene (propene).

4.7 The Ideal Gas Contribution

The Helmholtz energy of the ideal gas is given by

$$a^0 = h^0 - RT - Ts^0 \quad (2)$$

The ideal gas enthalpy is given by

$$\mathrm{h^0} = \mathrm{h_0^0} + \int_{\mathrm{T_0}}^{\mathrm{T}} \mathrm{c_p^0}\, \mathrm{dT} \quad (3)$$

$$\text{where } \mathrm{h_0^0} = \text{in J} \cdot \text{ mol} - 1 \text{ at } \mathrm{T_0}.$$

Where c_p^0 represents the ideal gas heat capacity and can be calculated using the following equation:

$$\frac{c_p^0}{R} = 4 + \sum_{k=3}^{6} v_k \, u_k^2 \frac{exp(u_k)}{[exp(u_k) - 1]^2} \quad (4)$$

Where R is the gas constant, R = 8.314472 J/mol·K, k = 3, 4, 5, and 6 series terms and represented respectively at v_3= 3.043, v_4= 5.874, v_5= 9.337, v_6= 7.922, v_7= 393 K/T, v_8= 1237 K/T, v_9= 1984 K/T, and v_{10}= 4351 K/T.

The ideal gas entropy is given by

$$s^0 = s_0^0 + \int_{T_0}^{T} \frac{c_p^0}{T} dT - R\, ln\left(\frac{\rho T}{\rho_0 T_0}\right) \quad (5)$$

where s_0^0 in $(\mathrm{J/\,mol \cdot\ K})$ at T_0.

Where $\rho_0$represents the ideal gas density and measured at $T_0 = 273.15\ K\ and\ P_0 = 0.001\ MPa$. Combining these equations results in the following equation for the Helmholtz energy of the ideal gas contribution:

$$a^0 = h_0^0 + \int_{T_0}^{T} c_p^0\, dT - RT - T\left[s_0^0 + \int_{T_0}^{T} \frac{c_p^0}{T} dT\ R\ ln\left(\frac{\rho T}{\rho_0 T_0}\right)\right] \quad (6)$$

The ideal gas Helmholtz energy is given in dimensionless form by

$$\alpha^0 = \frac{h_0^0 \tau}{RT_c} - \frac{s_0^0}{R} - 1 + \ln\left(\frac{\delta \tau_0}{\delta_0 \tau}\right) - \frac{\tau}{R}\int_{\tau_0}^{\tau} \frac{c_p^0}{\tau^2} d\tau + \frac{1}{R}\int_{\tau_0}^{\tau} \frac{c_p^0}{\tau} d\tau \quad (7)$$

Where $\delta_0 = \rho_0/\rho_c$ and $\tau = T_c/T$

The final ideal gas contribution after combining equations in the dimensionless form:

$$\alpha^0 = \ln \delta + 3\ ln\tau + a_1 + a_2\tau + \sum_{i=3}^{6} v_i\ ln[1 - exp(-b_i\tau)] \quad (8)$$

Where a_1= - 4.970583, a_2= 4.29352, b_3= 1.062478, b_4= 3.344237, b_5= 5.363757, b_6= 11.762957, and the values of v_k are the same represented previously. The values of $b_k$are equal to $u_k$divided by the critical temperature of the pure substance.

4.8 The Real Gas Contribution

The real gas contribution of the Helmholtz free energy is formulated as:

$$\alpha^r(\delta,\tau) = \sum_{k=1}^{5} N_k \delta^{d_k} \tau^{t_k} + \sum_{k=6}^{11} N_k \delta^{d_k} \tau^{t_k} exp(-\delta^{l_k}) + \sum_{k=12}^{18} N_k \delta^{d_k} \tau^{t_k} exp(-\eta_k(\delta - \varepsilon_k)^2 - \beta_k(\tau - \gamma_k)^2) \quad (9)$$

The real gas contribution part consists of three summation terms. The first term is the polynomial, that is written with N_k and exponents' terms. The exponents are d_k and t_k values and it is measured for all the 18 terms of the real gas contribution part (k=1 to k=18). In the second term, polynomial terms with exponential of dimensionless density powered by the Gaussian bell-shaped term $exp(-\delta^{l_k})$ which are explained in detail by Setzmann and Wagner for methane substance when they developed equation of state [9]. The primary use of Gaussian terms with t values equal and above k=6 is to represent the thermodynamics properties behavior of a substance near its critical point. Outside the critical region, the effect is dampened out with the δ^d contribution in the vapor phase and the $\exp(-\delta^l)$ part in the liquid phase. The coefficients and exponents of the Gaussian bell-shaped terms were fitted simultaneously with all the other parameters in the equation of state. The exponential terms are included that consist of a temperature dependency in the third term. This final piece allowed much lower values on the exponent t and provided a better physical representation behavior of the substance and possibly removed the creep two-phase state points. A complete detail on the values of each term of the real gas part is in appendix A.

4.9 Formula of Thermodynamic Properties

This concludes to the use of the Helmholtz free energy function to obtain thermodynamics properties using thermodynamics properties equation with the aid of PDE and ODE:

$$Z = \frac{P}{\rho RT} = \left(\frac{\partial a^r}{\partial\ \tau}\right)_\delta = \left(\delta\left(\frac{\partial a^r}{\partial\ \delta}\right)_\tau + 1\right) \tag{10}$$

$$p = \rho^2\left(\frac{\partial a}{\partial F}\right)_T \tag{11}$$

$$\frac{s}{R} = -\frac{1}{R}\left(\frac{\partial a}{\partial T}\right)_F \tag{12}$$

$$\frac{u}{RT} = \frac{a + Ts}{RT} = \tau\left[\left(\frac{\partial a^0}{\partial\ \tau}\right)_\delta + \left(\frac{\partial a^r}{\partial\ \tau}\right)_\delta\right] \tag{13}$$

$$\frac{h}{RT} = \frac{u + pV}{RT} = \tau\left[\left(\frac{\partial a^0}{\partial\ \tau}\right)_\delta + \left(\frac{\partial a^r}{\partial\ \tau}\right)_\delta\right] + \left(\delta\left(\frac{\partial a^r}{\partial\ \delta}\right)_\tau + 1\right) \tag{14}$$

5. Equation of State of Carbon Dioxide

Functional form of Equation of state of carbon dioxide in terms of Helmholtz energy (A) and written in the dimensionless form ϕ by Span and Wagner [7] as follows:

$$\phi\ (\delta, \tau) = \text{A } (\rho, \text{T})/\ \text{RT} \tag{15}$$

$$\phi\ (\delta, \tau) = \phi^0(\delta, \tau) + \phi^r(\delta, \tau) \tag{16}$$

Where ϕ^0= ideal gas behavior and ϕ^r = residual fluids behavior.

5.1 Ideal gas behavior $\boldsymbol{\phi^0}$

$$\phi^0(\delta, \tau) = \ln(\delta) + a_1^0 + a_2^0\tau + a_3^0 \ln(\tau) + \sum_{i=4}^{8} a^0 \ln[1\text{-}\exp(-\tau\theta_i^0)] \tag{17}$$

For the ideal gas at T=298.15 K and P = 0.101325 MPa, $a_1^0 + a_2^0$ are going to give zero due to the reference enthalpy and entropy calculations. All other data are given based on experimental work and details are tabulated by Span and Wagner [7].

5.2 The Residual Fluids Behavior $\boldsymbol{\phi^r}$

$$\phi^r(\delta, \tau) = \sum_{i=1}^{7} n_i\ \delta^{di}\ \tau^{ti} + \sum_{8}^{34} n_i\ \delta^{di}\ \tau^{ti}\ e^{-\delta^{ci}} + \sum_{35}^{39} n_i\ \delta^{di}\ \tau^{ti}\ e^{-\alpha i(\delta-\varepsilon i)^2 - \beta i(\tau-\lambda)^2} + \sum_{40}^{42} n_i\ \Delta^{\beta i}\ \delta\ \Psi \tag{18}$$

where Δ Is a linear optimization, Ψ is exponential term for fitting. All experimental data are also tabulated for the coefficients and variables given in the equation [9].

6. Equation of State of the Modified Benedict–Webb–Rubin (M. B.W. R.)

$$P=\rho RT+\rho^2[G(1)T+G(2)T^{1/2}+G(3)+G(4)/T+G(5)/T^2]+\rho^3[G(6)T+G(7)+G(8)/T+G(9)/T^2]$$
$$+\rho^4[G(10)T+G(11)+G(12)/T]+\rho^5[G(13)]+\rho^6[G(14)/T+G(15)/T^2]+\rho^7[G(16)/T]$$
$$+\rho^8[G(17)/T+G(18)/T^2]+\rho^9[G(19)/T^2]+\rho^3[G(20)/T^2+G(21)/T^3]\exp(\gamma\rho^2)$$
$$+\rho^5[G(22)/T^2+G(23)/T^4]\exp(\gamma\rho^2)+\rho^7[G(24)/T^2+G(25)/T^3]\exp(\gamma\rho^2)$$
$$+\rho^9[G(26)/T^2+G(27)/T^4]\exp(\gamma\rho^2)+\rho^{11}[G(28)/T^2+G(29)/T^3]\exp(\gamma\rho^2)$$
$$+\rho^{13}[G(30)/T^2+G(31)/T^3+G(32)/T^4]\exp(\gamma\rho^2).$$

This is a generalized version of the M.B.W.R. equation, where G (1) to G (32) are coefficients in form of (10^{-3}) and found in the appendix. For propane, they are further calculated in Ref. [6]. Below equations indicate the examples on how to calculate properties like enthalpy using the M.B.W.R. equation.

6.1 Enthalpy is Formulated According to the M. B.W. R. in the Following Form

$$H\ (T,\rho) = H^O + \frac{P-\rho RT}{\rho} + \left[\int_0^\rho \frac{P}{\rho} - \frac{T}{\rho^2}\left(\frac{\partial P}{\partial T}\right)\right] d\rho + \int_{T0}^{T} c_P^o dT$$
$$H^O = 11874.2\ \frac{J}{mol}\ at\ T^o = 298.15\ K\ and\ P = 0.101352\ MPa \tag{19}$$

$$c_v = c_P^0 - R\int_0^{P\rho} \frac{T}{\rho^2}\left(\frac{\partial P}{\partial T}\left(\frac{\partial P}{\partial T}\right)\right) d\rho \tag{20}$$

The enthalpy data is tabulated at non-isothermal and non-isobaric process for the saturated liquid-vapor enthalpy and superheated vapor enthalpy in “Fundamentals of Engineering Thermodynamics” [11].

7. Equation of State for Mixtures of Fluids

In mixtures, such as propane with carbon dioxide, the Helmholtz free energy equation of state is derived as similar with the addition of the composition functionality by Kunz and Wagner [20]. This requires rewriting the equation of state using the Helmholtz free energy as a function of density, temperature and composition and given the functional form of EOS of mixtures by Kunz and Wagner [20].

$$\alpha(\delta, \tau, \overline{x}) = \alpha^0(\delta, \tau, \overline{x}) + \alpha^r(\delta, \tau, \overline{x}) \qquad (21)$$

$$\overline{x} \text{ is the molar mass composition}$$

Where δ is reduced mixture density i.e. $\delta = \rho/\rho_r$, τ is the inverse reduced mixture i.e. $\tau = T_r/T$ with $\rho_r = \rho_r(\overline{x})$ and $T_r = T_r(\overline{x})$.

7.1 Dimensionless form for ideal gas mixture is given by

$$\alpha^0(\delta, \tau, \overline{x}) = \sum_{i=1}^{N} x_i[\alpha_{0i}^0(\rho, T) + \ln x_i] \qquad (22)$$

Summation of Helmholtz ideal gas mixture contribution is given two terms. The N accounts for the total components of mixture and α_{0i}^0 is the dimensionless form of the Helmholtz free energy in the ideal-gas state of component i. The x_i is the mole fractions of the mixture constituents. The "ln" account for entropy mixing that is the term $x_i \ln x_i$ represents for the entropy of mixing for each x_i in the mixture.

7.2 Dimensionless form for residual part for the mixture is given by

$$\alpha^{r}(\delta,\tau,\overline{x}) = \sum_{i=1}^{N} x_i \alpha_{0i}^{r}(\delta,T) + \Delta\alpha^{r}(\delta,\tau,\overline{x}) \tag{23}$$

Where α_{0i}^{r} is the residual part of the reduced Helmholtz free energy of component i and $\Delta\alpha^{r}$ is the departure function that reduced the residual Helmholtz free energy and is given as follows:

$$\Delta\alpha^{r}(\delta,\tau,\overline{x}) = \sum_{i=1}^{N-1}\sum_{j=i+1}^{N} \Delta\alpha_{ij}^{r}(\delta,\tau,\overline{x}) \tag{24}$$

$$\Delta\alpha_{ij}^{r}(\delta,\tau,\overline{x}) = x_i x_j F_{ij} \alpha_{ij}^{r}(\delta,\tau) \tag{25}$$

The parameter Fij equals unity for binary specific departure functions. The term $\alpha_{ij}^{r}$is introduced with parameters depending on the mixture, for more details see [20].

7.3 The Enthalpy of A Mixture is Given by

$$\frac{h\,(\delta,\tau,\overline{x})}{RT} = 1 + \tau(\alpha_{\tau}^{O} + \alpha_{\tau}^{r}) + \delta(\alpha_{\delta}^{r}) \tag{26}$$

8. Comparison Between Equations of States

It is critically important to have the most accurate EOS, since all thermo-physical properties of the gases are determined using it. So, in this section a comparison of the results of Helmholtz energy-based EOS, which is used by REFPROP, with the M.B.W.R. EOS results which is widely used in textbooks is discussed.

8.1 Comparison Methodology

The results of NIST EOS are analyzed and compared with EOS of M.B.W.R. for the case of Hydrocarbons, while comparing NIST EOS with Sandia EOS for the case of pure (CO_2). A tabular form using MBWRE for thermodynamic properties calculation is presented (Table: A16-A18) [11]. The comparison of both EOS studies the enthalpy at non-isothermal process with isobaric process. Later on, a study on the non-isothermal and non-isobaric process is conducted. In addition, the results are further investigated with their uncertainties to seek and obtain the most efficient EOS that should be used in hereafter when analyzing systems that are enthalpy-based.

8.2 Temperature and Pressure Factors

The temperature and pressure are considered at the operating conditions at which the system operates. The temperature ranges from to the maximum operating temperature. The assumed operating conditions of the vapor compression refrigeration system (VCRS) are as follows: non-isothermal/isobaric compression process, isobaric processes, and non-isothermal expansion process, and isobaric process. In this study, comparison of both EOSs is conducted at isobaric process with varying the temperatures from a temperature of (270 K) to temperature of (340K). In addition, another comparison is presented for saturated liquid-vapor curve at non-isobaric process. Lastly, comparison of both equations is presented at isobaric process (P = 1 bar) for the superheated vapor enthalpy of propane.

9. Results and Discussions of EOSs

9.1 Saturated Liquid-Vapor Enthalpy Test (Non-Isobar Test)

Non-isothermal process has been applied at constant pressure of propane. The accuracy test was performed using the NIST EOS and the MBWR equation of state at temperature ranges from (270 K) to near the critical temperature (360 K) of the propane. In this range of temperature and pressure, the propane exists at saturated liquid-vapor curve where measurements of saturated liquid and vapor enthalpy have been conducted. The results are tabulated and plotted accordingly.

Table 6: Enthalpy calculations using NIST and MBWR EOS of propane.

T (K)	NIST: enthalpy of sat. liquid (J/mole)	NIST: enthalpy of sat. vapor (J/mole)	MBWR: enthalpy of sat. liquid (J/mole)	MBWR: enthalpy of sat. vapor (J/mole)
270	- 4581	12140	-4726	11970
280	-3472	12623	-3609	12460
290	-2327	13084	-2523	12920
300	-1142	13517	-1262	13360
310	89	13914	-20	13760
320	1377	14261	1276	14120
330	2733	14540	2641	14410
340	4180	14717	4096	14610
350	5760	14723	5686	14640
360	7589	14389	7528	14340

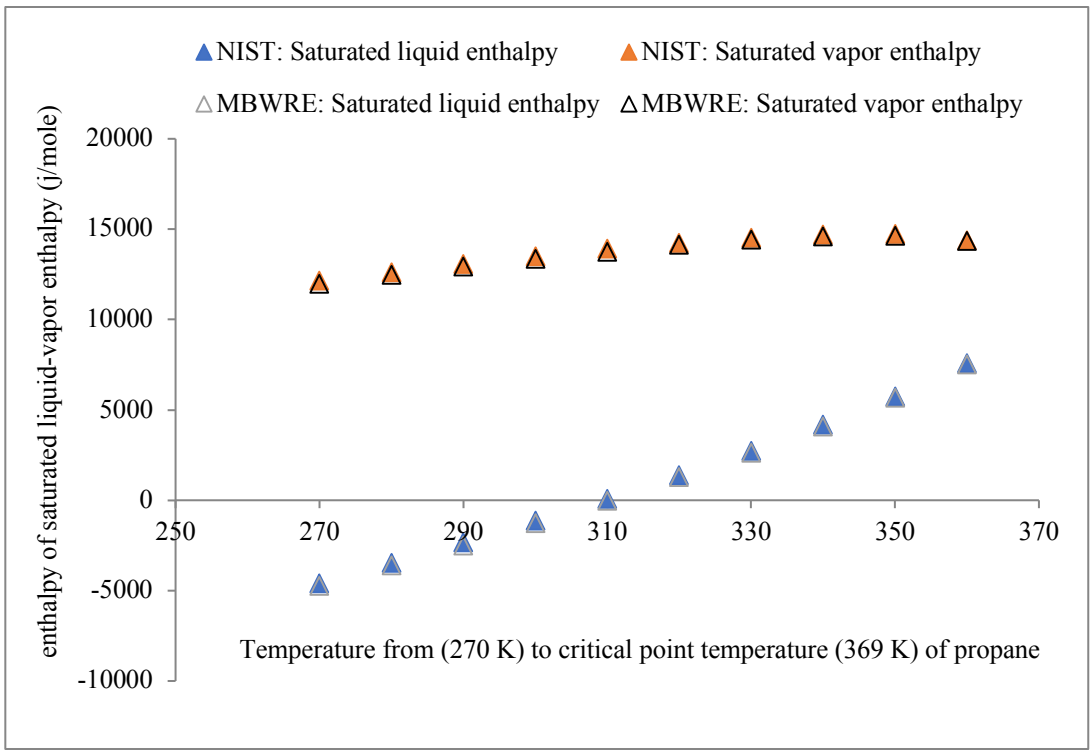

Figure 3: Enthalpy as a function of temperature using two EOSs of NIST and MBWRE of propane.

9.2 Isobar Enthalpy Test

Another non-isothermal process has been applied at constant pressure of propane. The accuracy test was performed using the same NIST and MBWR EOS at temperature ranges from (200 K) to temperature of (340 K). The pressure selected at (P = 0.101 MPa), to maintain isobar process. In this range of temperatures, the propane exists at the superheated vapor region of the T-S diagram where measurements of superheated enthalpy have been performed. The results are tabulated and plotted accordingly. These results are based on experimental studies conducted on [7] and [1].

Table 7: Enthalpy of superheated region using NIST and MBWR EOS of propane at $P = 0.101$ MPa

T (K)	MBWR: enthalpy (J/mole)	NIST: enthalpy (J/mole)
200	-11780	-11617
235	10220	10390
240	10550	10712
260	11890	12035
280	13280	13421
300	14750	14878
320	16290	16408
340	17910	18014

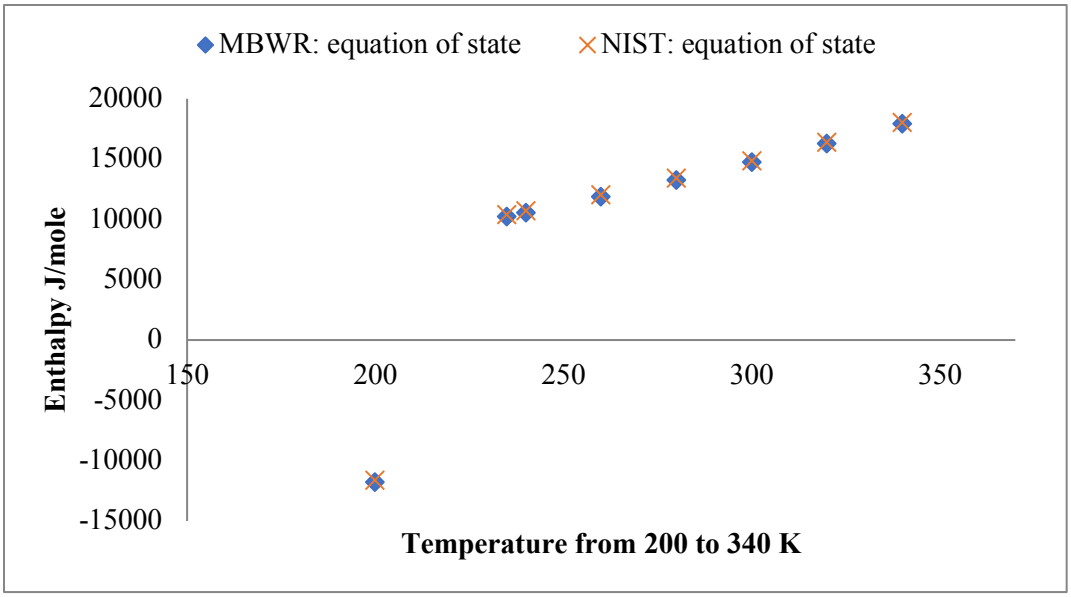

Figure 4: Enthalpy as a function of temperature using two EOSs of NIST and MBWR of propane at P= 0.101325 MPa.

9.3 Isobar Enthalpy Test

Non-isothermal process has been applied at constant pressure of carbon dioxide (CO_2). The accuracy test was performed using the same EOS of NIST but compared to Sandia EOS at temperature ranges from (200 K) to temperature of (600 K). The pressure selected at (P = 0.101 MPa), to maintain isobar process. In this range of temperatures, the carbon dioxide (CO_2) exists at the superheated vapor region of the T-S diagram where measurements of superheated enthalpy have been performed. The results are tabulated and plotted accordingly. These results are based on experimental studies conducted by NIST and Sandia experimental labs in which it demonstrates the capability of NIST EOS at the superheated region measurements as accurate database.

Table 8: Enthalpy calculations using NIST EOS and Sandia EOS of carbon dioxide.

T (K)	NIST 1996 EOS enthalpy (kJ/kmole)	Sandia 1994 EOS enthalpy (kJ/kmole)
200	-3482	-3423
300	70	69
400	4024	4003
500	8336	8301
600	12943	12899

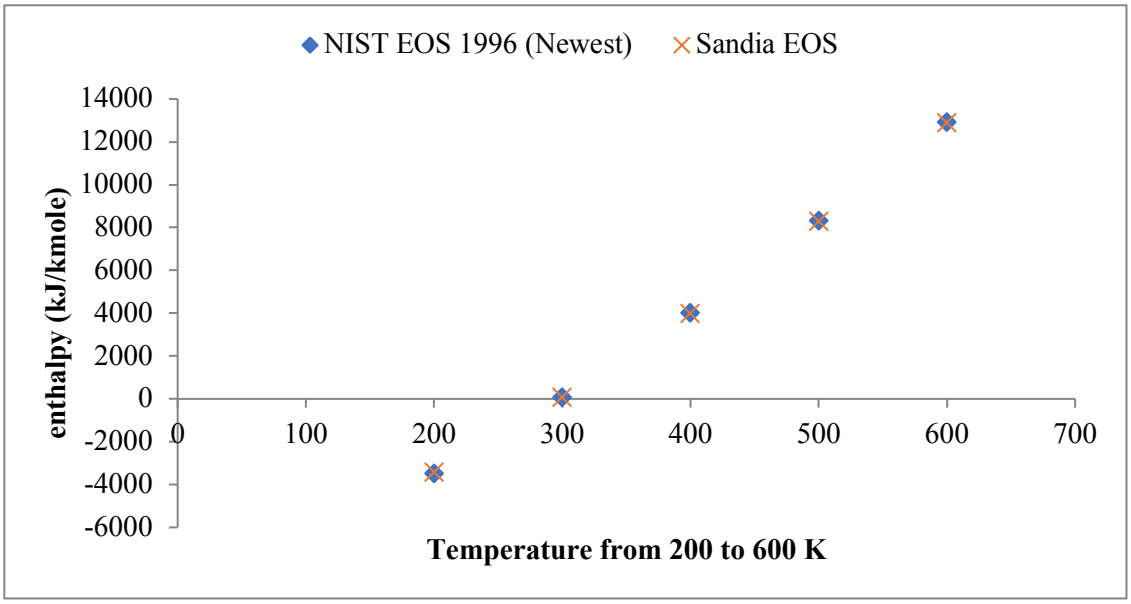

Figure 5: Enthalpy as a function of temperature using NIST and Sandia EOSs for carbon dioxide at P = 0.101325MPa.

9.4 Saturated Liquid-Vapor Enthalpy Test (Non-Isobar Test)

Non-isothermal process has been applied at non-isobaric pressure of carbon dioxide (CO_2). The accuracy test was performed using the NIST 1994 EOS and NIST 1994 EOS at temperature ranges from (220 K) to near the critical temperature (304.13 K) of the (CO_2.). In this range of temperature and pressure, the carbon dioxide exists at saturated liquid-vapor curve where measurements of saturated liquid-vapor enthalpy have been conducted. The results are compared to demonstrate NIST 1994 EOS with 1996 EOS for which is more accurate since it has fewer uncertainties.

Table 9: Enthalpy calculations using NIST 1996 and 1994 EOS of carbon dioxide.

T (K)	NIST 1996: enthalpy of sat. liquid (kJ/kg)	NIST 1996: enthalpy of sat. vapor (kJ/kg)	NIST 1994: enthalpy of sat. liquid (kJ/kg)	NIST 1994: enthalpy of sat. vapor (kJ/kg)
220	-419	-74	-420	-75
250	-358	-68	-359	-69
272	-308	-74	-309	-75
290	-260	-92	-261	-93
300	-222	-118	-223	-119
304	-187	-157	-188	-158
304.13	-173	-173	-174	Critical point

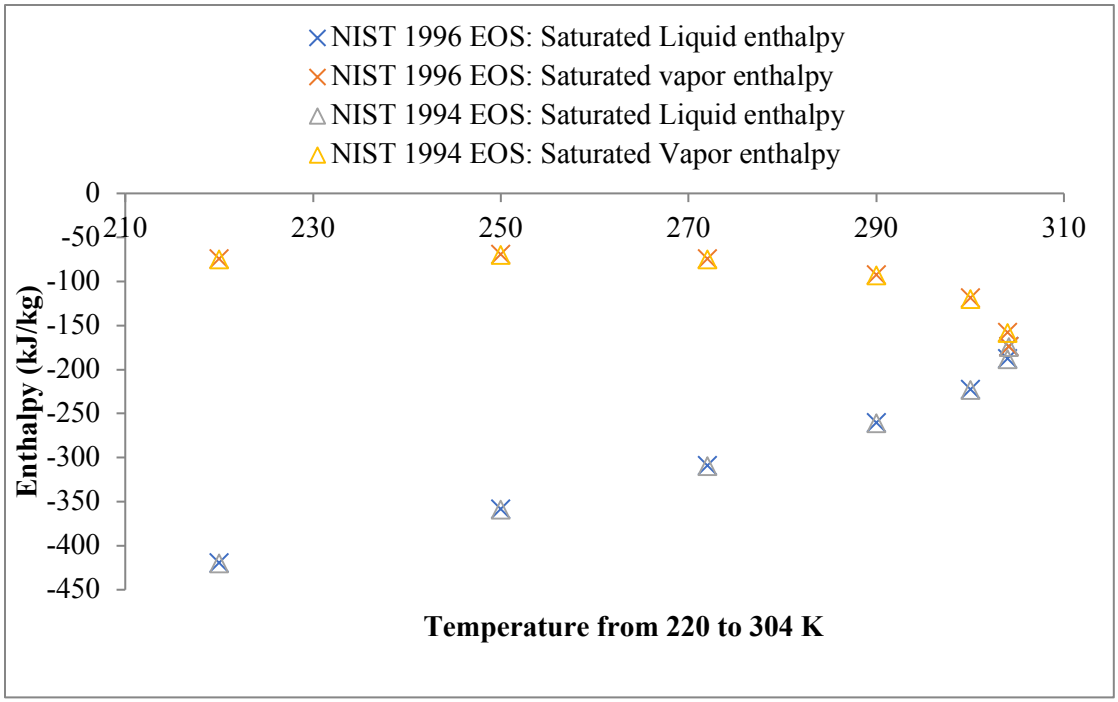

Figure 6: Enthalpy of saturated liquid and vapor as a function of temperature using two EOSs of carbon dioxide.

9.5 Isobar Enthalpy Test

Non-isothermal process has been applied at moderate and elevated pressures of carbon dioxide (CO_2). The accuracy test was performed using the NIST EOS 1994 and 1996 at temperature ranges from (480 K) to temperature of (700 K). The pressure selected at moderate pressure (P = 10 MPa), to maintain isobar process. In this range of temperatures, the carbon dioxide (CO_2). exists at the supercritical vapor region of the T-S diagram where measurements of supercritical enthalpy have been performed. These results are also based on experimental studies conducted by NIST experimental lab in which they demonstrate the capability of NIST EOS at the supercritical region measurements as accurate program database.

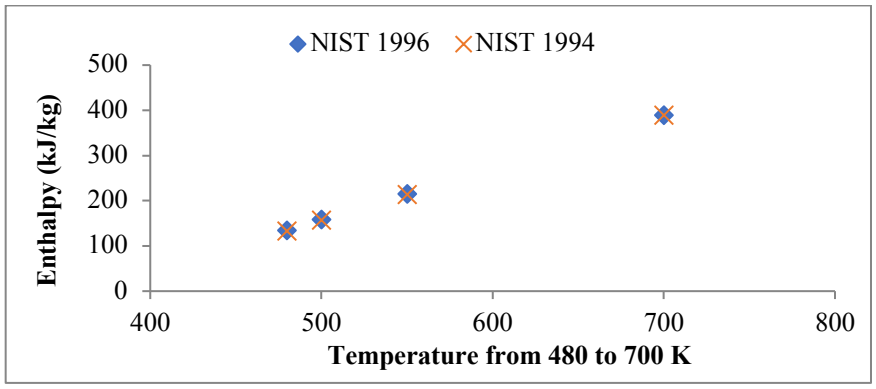

Figure 7: Enthalpy as a function of temperature of supercritical region of carbon dioxide at P = 10 MPa.

9.6 Isobar process at elevated pressure (P = 15 MPa)

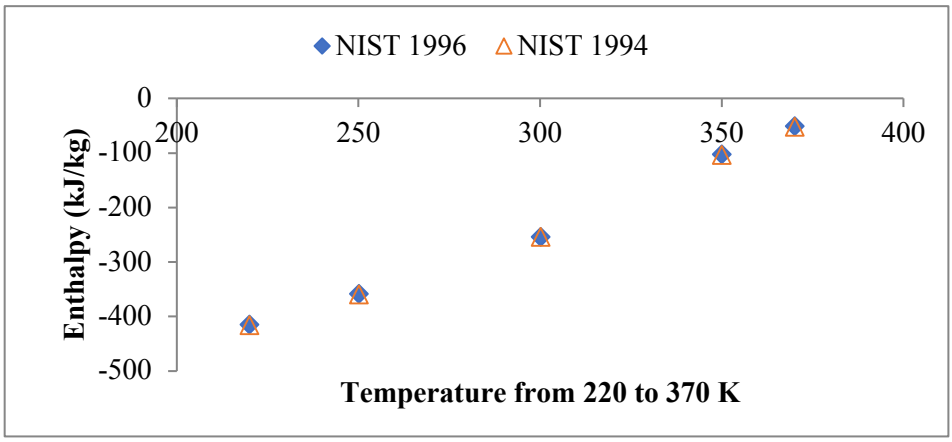

Figure 8: Enthalpy as a function of temperature of supercritical region of carbon dioxide at P = 15 MPa.

9.7 Conclusion on the Two Equations of States

Evaluation of the capability of the MBWR equation for predictions of the saturated liquid-vapor and superheated vapor thermodynamic properties of the propane was conducted by comparing the enthalpy results. The MBWR enthalpy values [6] are compared with the Lemmon and Wagner [7] enthalpy equation, namely NIST EOS. According to the plots of saturated liquid-vapor enthalpy, it can be seen that the NIST results of saturated liquid-vapor enthalpy follow the same trend as the MBWR. However, both data of the saturated liquid-vapor enthalpy show a small difference. For instance, in the saturated liquid curve, NIST provides enthalpy above the enthalpy provided by that in MBRW Eq. This difference is in the range of 100 (J/mole) that makes up of approximately less than 2 % of a possible error. Similarly, the enthalpy of saturated vapor using NIST shows similar trend with MBRW enthalpy of saturated vapor results with approximately 104 additional (J/mole) than using the NIST EOS. These differences are due to the less accuracy of the MBRWE [6] where its enthalpy parameters have uncertainty for propane within (1%).

The equation of state by Younglove and Ely (MBRW Eq.) is a 32-term but lucks the exponential and fitting terms. The MBRW Eq. is indeed a good approximation for finding the trend of a pure substance at different temperatures. However, Lemmon and Wagner (NIST equation of state) has provided several correcting and fitting terms that makes the equation of state of pure substance more accurate than those equation used prior to 2008. These equations prior to 2008 suffer from several shortcomings according to Lemmon and Wagner [7] as follows:

1. Data for propane are not considered in the range of their experimental uncertainties.
2. Unacceptable behavior shown by some EOS where experimental data were not available.
3. The two-phase region resulted in enormous values caused by large exponents in the EOS terms. For detailed justifications of the validation of NIST EOS, see Lemmon and Wagner [7].

9.8 Mathematical Gaps of NIST Equations of State

Following reading articles that focus on the mathematical error reduction on equation of state, NIST obtained an accurate equation of state that has the least error and is been recently published [7]. The error in obtaining speed of sound is 0.01% below 350 K in the vapor phase up to pressure 1MPa and 0.03% in the liquid phase for temperature (260-420 K) [7]. The liquid phase value also applies at temperatures greater than 350 K (to nearly 500 K) at pressures above 10 MPa. Uncertainty in vapor pressure is 0.03% for temperature above (180 K).

9.9 Formulating the Functional Code

Both equations of state can be used to find the trend of the thermodynamics properties but only the NIST EOS showed better fitting terms and good approximation of the thermodynamics properties. The NIST EOS is incorporated in NIST REFPROP 9.1 software in the form of mathematical code [4] and [5]. This mathematical code is used to measure thermodynamics properties accurately at any equilibrium state, sub-cooled region or superheated region, whether in the single-phase or multi-phases. NIST developers suggest using the default option since the default option calculates thermodynamics properties on substance-based EOS. Recent optimization with accurate mathematical terms has been added to the NIST EOS to reduce errors [7]. The default option is used for either pure substance or a mixture with different EOS (different code) and measures the thermodynamics properties. As a result, the NIST REFPROP 9.1 will be used as a reference for obtaining thermodynamics properties data and simulate these data with the aid of MATLAB code.

10. Mixture Analysis at Different Conditions

In order to choose the operational conditions, an assessment of the performance for each mixture is needed. As the evaporator temperature (outlet) is assumed to be saturated vapor, the enthalpy of saturated vapor at which the evaporator operates is conducted at multiple temperatures. In this procedure, determining the results of the enthalpy of saturated vapor of each mixture varying with temperatures is taken as the first priority for choosing the evaporator temperature. In other words, the compressor work formulated as a function of the saturated vapor of evaporator outlet (h_g) in which it can be selected at an appropriate enthalpy for each specific mixture. Figure 9 shows the enthalpy of saturated vapor as function of (CO_2) at different temperatures for propane. Figure 10 shows the enthalpy of saturated vapor as function of (CO_2) at different temperatures for n-buatne. Figure 11 shows the enthalpy of saturated vapor as function of (CO_2) at different temperatures for dimethyl ether. Figure 12 shows the enthalpy of saturated vapor as function of (CO_2) at different temperatures for propylene. In addition, the enthalpy versus entropy is analyzed for each mixture to show the effect of (CO_2) at the chosen temperatures. Furthermore, the Pressure-x CO_2 Figures have been performed as the mole fraction of (CO_2) increases corresponding to the evaporator temperatures. The Pressure-x CO_2 Figures for each refrigerant are inserted in appendix C. According to the Figures of h_g-x(composition) for all the mixtures indicated, as the temperature decreases, decline of the enthalpy of saturated vapor is noticed. According to Figures 9, this declination has a crossover point at 70 % mole fraction of CO_2 for temperature range of – 4 to 30 ℃ degrees for propane.

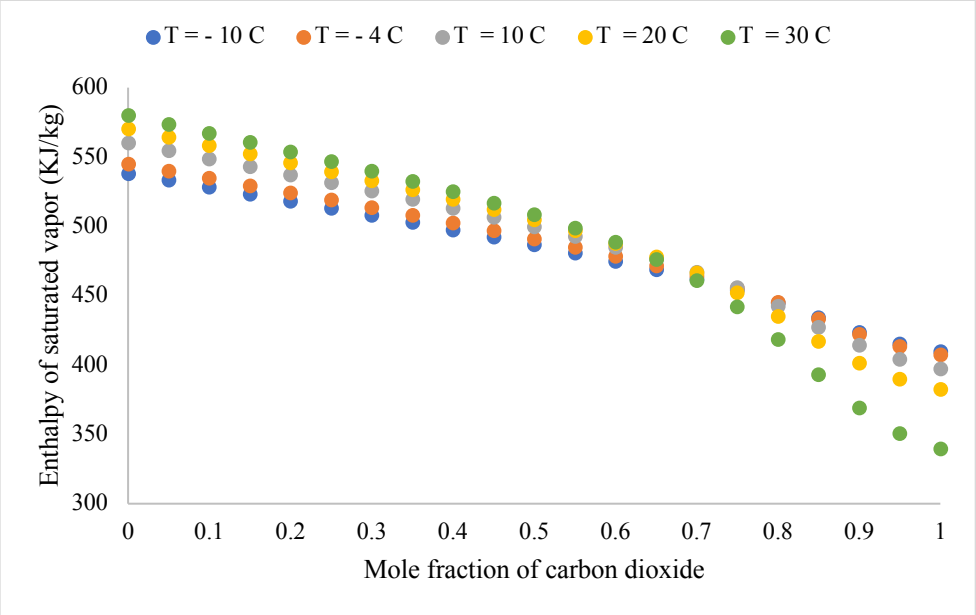

Figure 9: Enthalpy of saturated vapor as a function of carbon dioxide.

For the same temperature range, the propylene has crossover points occurring at 70 % mole fraction of CO_2 as they have similar critical value of temperatures based on Figure 10. It is noticed that the cross points occurring at different mole fractions of (CO_2) is because of the thermophysical properties of the refrigerants, the higher the critical temperatures, the further the crossover point.

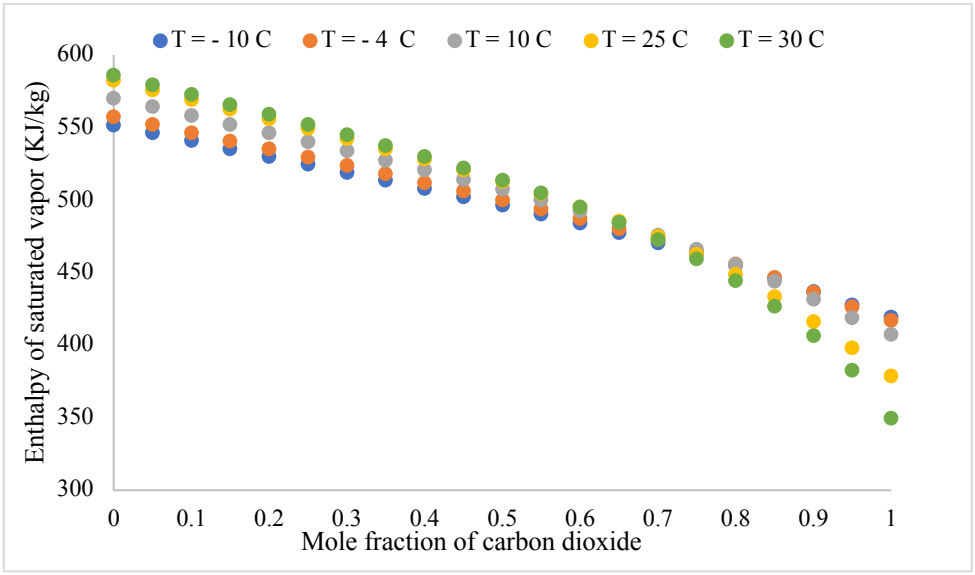

Figure 10: Enthalpy of saturated vapor as a function of carbon dioxide.

Additionally, the n-butane has further crossover points occurring at 90 % mole fraction of CO_2 according to Figure 11. It is worth mentioning that the cross points occurring at different mole fractions of CO_2 is mainly because of the thermophysical properties of the refrigerants, the higher the critical temperatures, the further the crossover point. For these blends, the enthalpy of saturated vapor (h_g) is appropriately chosen before the crossover point in order to overcome the sever declination revolving after this cross-over point. The higher h_g indicates the smaller compression work require, thus obtaining higher COP for fixed heat absorbed Q_{evp}.

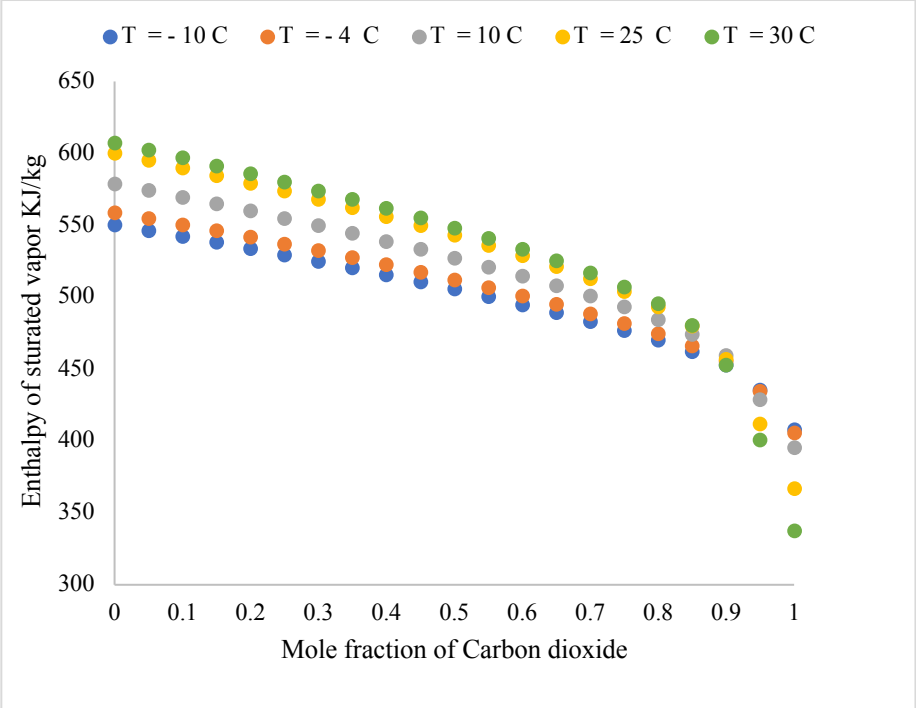

Figure 11: Enthalpy of saturated vapor as a function of carbon dioxide.

Figure 12 indicates that the dimethyl ether (h_g) is approximately similar at all CO_2 mole fractions up to the crossover point which indicates this blend is suitable for systems with high volumetric capacity concerns. The only issue for these blends prior to their crossover points is their flammability at smaller mole fractions of CO_2 than that of hydrocarbons mole fractions.

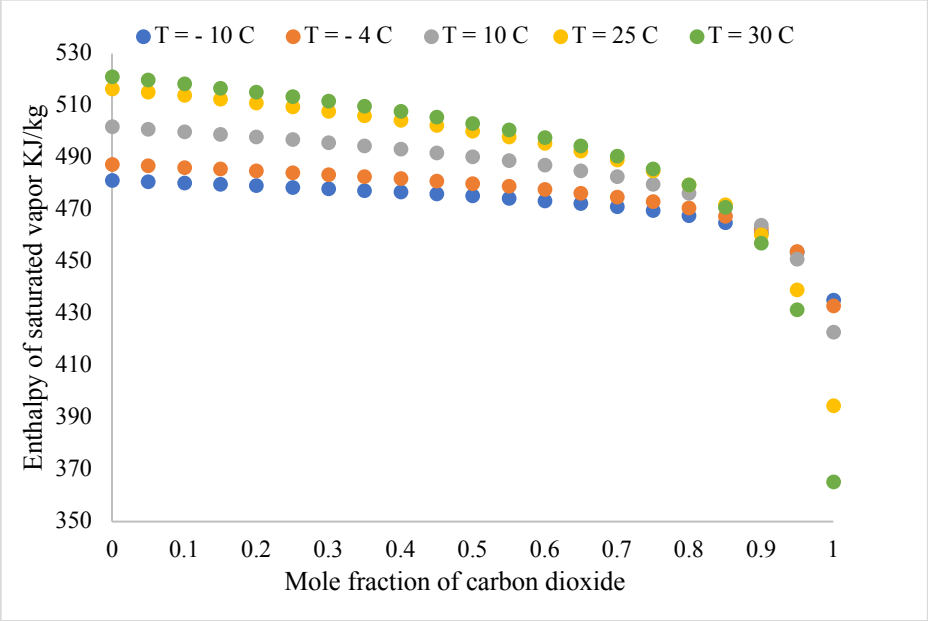

Figure 12: Enthalpy of saturated vapor as a function of carbon dioxide.

The enthalpy of saturated vapor versus entropy of saturated vapor (h_g-s_g) graphs for each mixture are also analyzed. This analysis is conducted to see the vapor entropy s_g changes when choosing the appropriate h_g as well as to see the effect of the carbon dioxide. As seen in Figure 13, as the temperature decreases, the saturated vapor entropy s_g shows increase in a curved-vertical shape with (CO_2) mole fractions for propane. Also, Figure 14 shows sharp decline on the dimethyl ether comparing to n-butane with carbon dioxide mixture at the same range of temperatures.

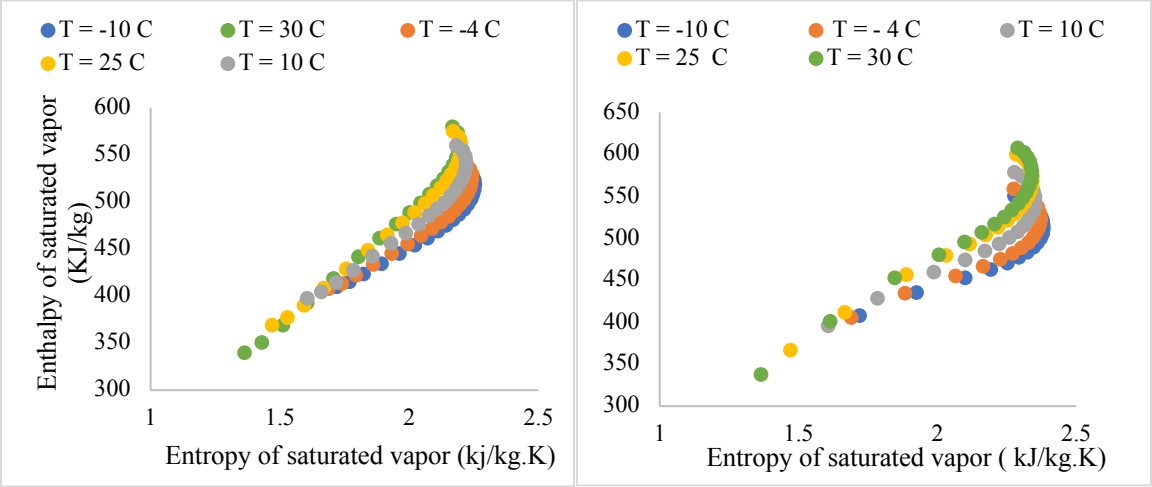

Figure 13: Entropy of saturated vapor as a function of carbon dioxide for propane (left) and n-butane (right)

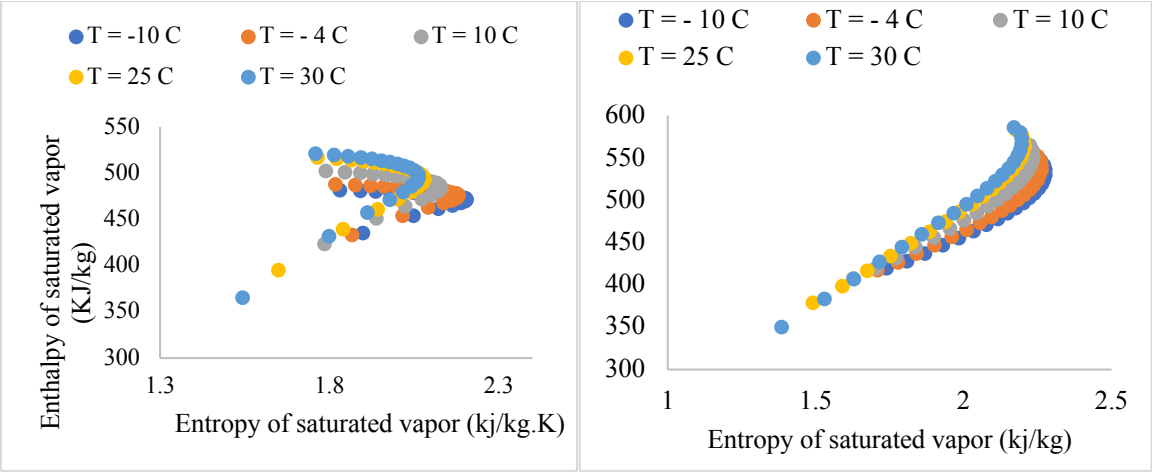

Figure 14: Entropy of saturated vapor as a function of carbon dioxide for dimethyl ether (left) and propylene (right)

11. Mixtures at Constant Temperatures and Constant Pressures

In order to draw a clear conclusion for changes with CO_2 mole fractions, a constant temperature vs. CO_2 mole fractions are analyzed. This analysis is conducted to illustrate the behavior of the mixture at the liquid, liquid-gas, and gaseous phases. The pressure has been chosen between pressure range of 100 kPa to 5000 kPa. For fluids at gaseous phase, the phase change to liquid-gas phase (two-phase) occurring when pressure is elevated at constant temperature. High enough pressure result in a phase change to liquid phase such as at P = 4000, 5000, and 6000 kPa. The case of propane-x CO_2 is taken for illustration purposes. All other mixture is analyzed and inserted in the appendix. According to Figure 15, at high constant pressure, the constant temperature behavior of mixture exhibits all phases; liquid, liquid-gas, and gaseous phases. This is called solubility of mixture. At specific temperature and pressure on the T-Composition and P-Composition, there is a corresponding mole fractions called solubility. As an illustration, at the dew point temperature, the mole fraction of vapor is the solubility of liquid constituent in gaseous constituent. At the bubble point, the mole fraction of liquid is the solubility of vapor constituent in liquified constituent [14]. This enables the mixture to change from the saturated liquid to saturated vapor phase (evaporate) due to the higher vapor pressure (higher volatility) of liquid as well as the higher mole fractions of vapor constituent at a given temperature and pressure.

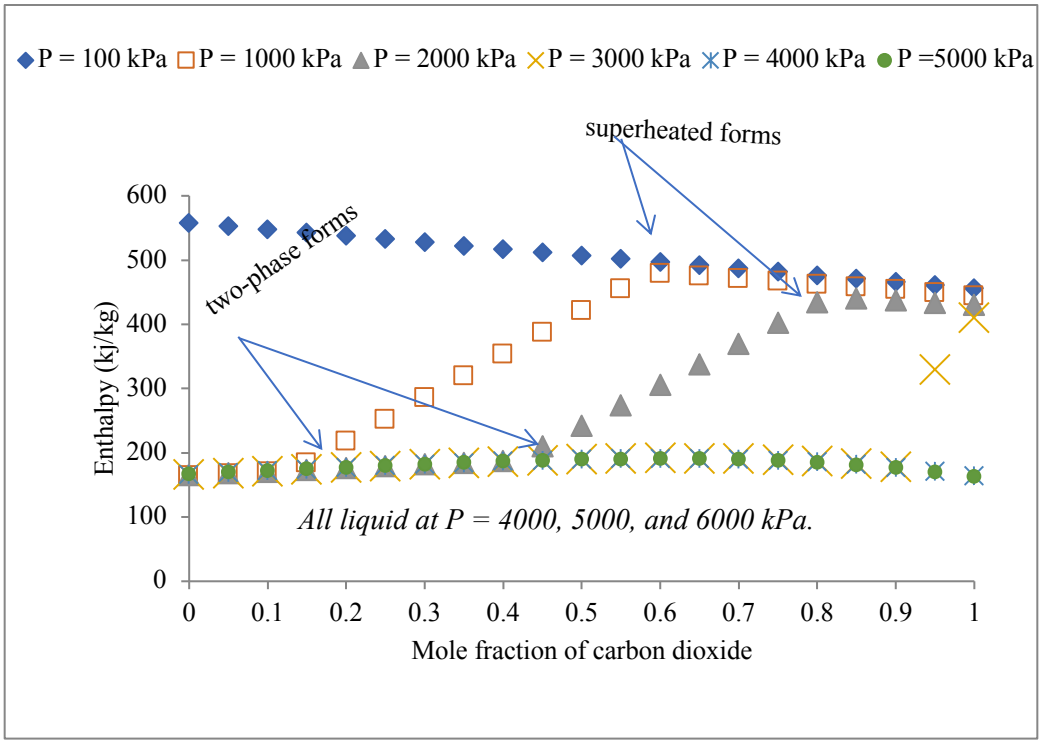

Figure 15: Enthalpy as a function of carbon dioxide at constant T = - 4 ℃.

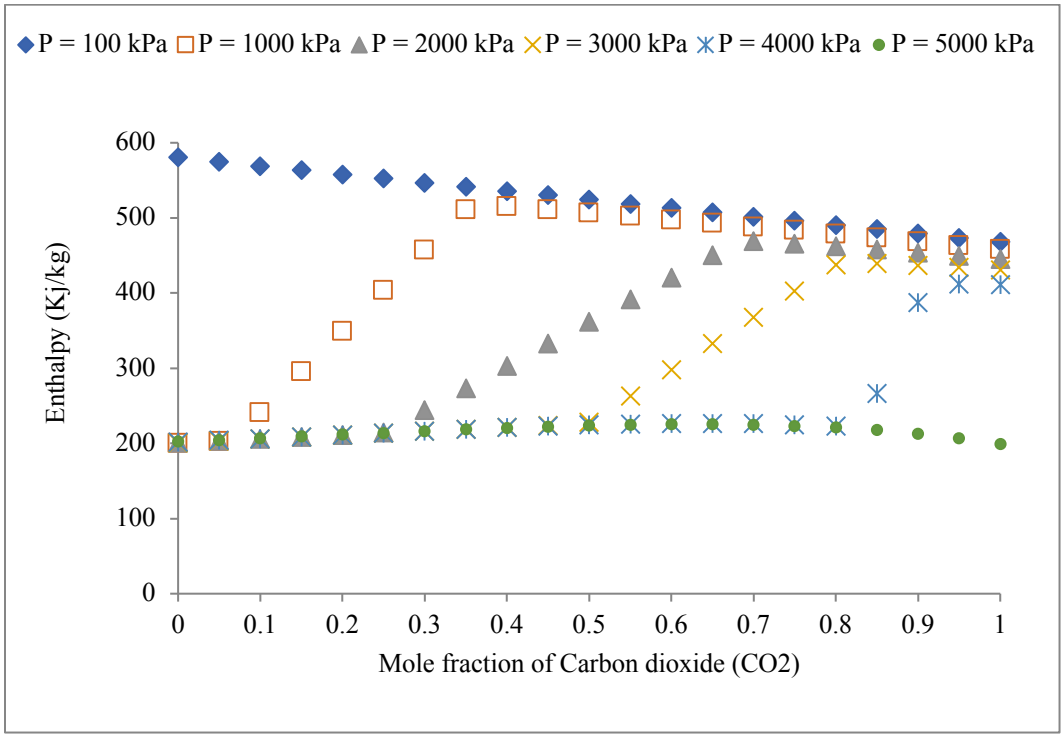

Figure 16: Enthalpy as a function of carbon dioxide at constant T = 10 ℃.

12. Volumetric Capacity of Mixture

The volumetric capacity of the system is a function of the rate of energy (heat) transfer in the evaporating device with respect to the specific volume passing the device. The volumetric efficiency is assumed to be 100 %. The hydrocarbons-carbon dioxide blends are studied at the chosen operating conditions to evaluate the change of specific volume upon (CO_2) additions. The mixtures volume decreases as the (CO_2) concentration increases. This decrease enhances the volumetric capacity of the cycle upon mixing with (CO_2) mole fractions.

Figure 17 shows the volume of propane when mixing with (CO_2). The volumes decrease upon the addition of (CO_2) mole fractions in which it shows that the volumetric capacity at certain heat (energy) transfer of evaporator would improve. The propane has higher volume than propylene and thus propylene would then have higher volumetric capacity at certain heat (energy) transfer of evaporator according to Figure 17.

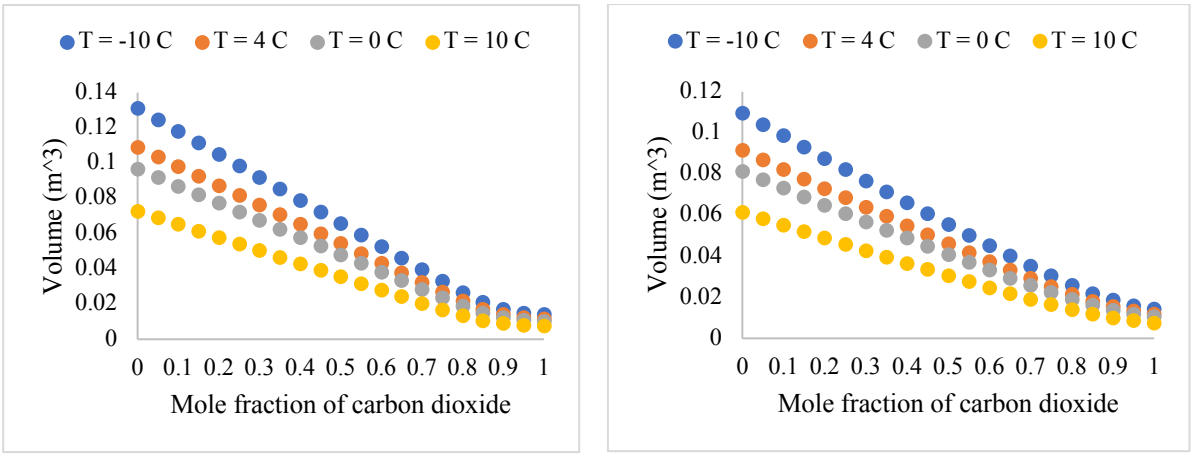

Figure 17: Volume as a function of carbon dioxide for propane (left) and propylene (right).

On the contrary, Figure 18 demonstrates that the n-butane has higher volumes upon mixing with (CO_2) mole fractions. These high volumes lower the volumetric capacity of this binary mixture. For n-butane, the mixing process with (CO_2) concentrations does not improve the volumetric capacity that much comparing to the propane and propylene. The dimethyl ether shown in Figure 18 has better volumes upon mixing with (CO_2) concentrations and thus the volumetric capacity is acceptable comparing to n-butane.

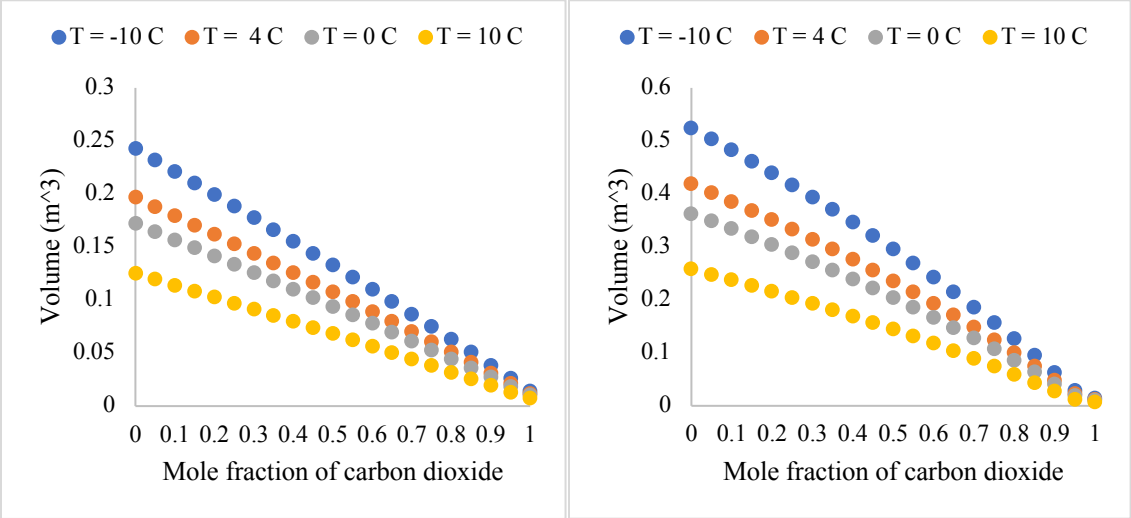

Figure 18 : Volume as a function of carbon dioxide for dimethyl ether (left) and n-butane (right).

13. Thermodynamic Cycles

In 1834, Jacobs Perkins [19] used pure refrigerants in the first vapor compression system that uses the compression work to transfer energy between the heat sources to the heat sink. The system used ammonia, sulphureted dioxide, and methyl-chloride as the main working fluids until 1930. The concept of replacing pure refrigerant by a mixture was first introduced in 1885 by Pictet [19] by utilizing a volatile liquid that spilt up into one or more liquids within the system. The vapor compression system operates on the well-known reverse Rankine cycle in which a refrigerant undergoes phase change in the condensation and evaporation processes. It is worthwhile to notice that in the revers Rankine cycle, the compressor inlet is vapor (vaporized) and the condenser outlet is fully liquefied (condensed). In the early work of air conditioning, Carnot cycle provides a limit of the highest possible achievement and is used as the reference for refrigeration and heat pump cycles.

13.1 Carnot Cycle

Carnot cycle consists of compressor, condenser, turbine, and evaporator. The compressor undergoes isentropic process to provide the maximum work to transfer the energy between the heat source and the heat sink. In the condensation process, the condenser rejects the energy (heat) of condensation to an external heat sink at isobaric process and temperature namely Tc. In the following process, the turbine expands in isotropic process where it brings the working fluids from elevated pressure and temperature to that of the evaporation working temperature and pressure. In the evaporation process, the fluids undergo isobaric process where it vaporizes the fluids. In this way, the efficiency of the compressor and the evaporation is 100 % each and thus coefficient of performance (COP) is the ideal (COP) that can be obtained for such a fluid. Due to practical difficulties in the compressor design such as the difficulty of achieving isothermal compression and the presence of liquid that requires wet compression, the compressor needed to be redesigned. Also, due to nature of liquid entering the turbine that has lower specific volume than that of vapor. The turbine is replaced with a throttle valve to avoid practical difficulties of the Carnot cycle led up to the well-known reversible reverse Rankine cycle invented by Pictet [19].

13.2 Reverse Rankine Cycle

The reversible reverse Rankine cycle consists of compressor, condenser, throttle, and evaporator. The throttle valve is by default has irreversibility and those it requires more compressor work and as a result it affects the (COP) of the cycle. The throttle valve process is isenthalpic process where the fluids keep it is enthalpy constant. The compressor undergoes isentropic process to provide the maximum possible work to transfer the energy between the heat source and the heat sink. In the condensation process, the condenser rejects the energy (heat) of condensation to an external heat sink at isobaric process and temperature Tc. Later on, process, the throttle valve expands in non-isotropic and isenthalpic process where it brings the working fluids from elevated pressure and temperature to that of the evaporation working temperature and pressure. In the evaporation process, the fluids undergo isobaric process where it vaporizes the fluids at temperature (Te). In reverse Rankine cycle, the efficiency of the compressor and the evaporation is 100 % each. However, due to the irreversible throttle process it lowers the coefficient of performance (COP). This is assumed to be the ideal (COP). In real case, the obtained (COP) later compared to this (COP) of reverse Rankine cycle for such a fluid. Additional to the four components is the energy (heat) exchanger where it provides a means of sub-cooling in which the energy exchanger transfers the energy (heat) between the condensers and heats up the compressor inlet. With the aid of the energy (heat) exchanger, the compressor is protected from the two-phase flow existing from the evaporator. Of course, the inlet of the compressor will shift to the superheated region in which it reduces the amount of work required by the compressor. Hence, the performance of the operating cycle would improve for fluids having high heat capacity and low (COP) [19]. For mixtures, the Lorentz cycle is considered in this work. The Lorenze consists of the same components and due to fact that mixtures exhibit a temperature glide (TG) during condensation and evaporation processes, the Lorenze cycle illustrate this drop and thus it is adopted in this thesis in the case of mixture as the working fluids.

13.3 Assumptions Made on the Thermodynamic Cycle

The refrigeration system consists of compressor condenser, expansion valve, and evaporator. In order to facilitate the analysis procedures, the following assumptions were introduced:

1. The compressor isentropic efficiency is assumed to be 85 % for the unitary refrigeration system whereas the energy (heat) exchangers such as the evaporator and condenser are assumed to undergo isobaric process.
2. The expansion valve is assumed to be isenthalpic.
3. The energy (heat) transfers and pressure loss in the flowing pipes are negligible.
4. Saturated vapor is assumed at the exit of evaporator and saturated liquid at the exit of condenser is also assumed.
5. For unitary refrigeration system, the saturated vapor temperature is assumed to be – 15, $-4, +4$ ℃ degrees where the saturated liquid temperature is taken at 25 and 45 ℃, namely operating at room temperatures.

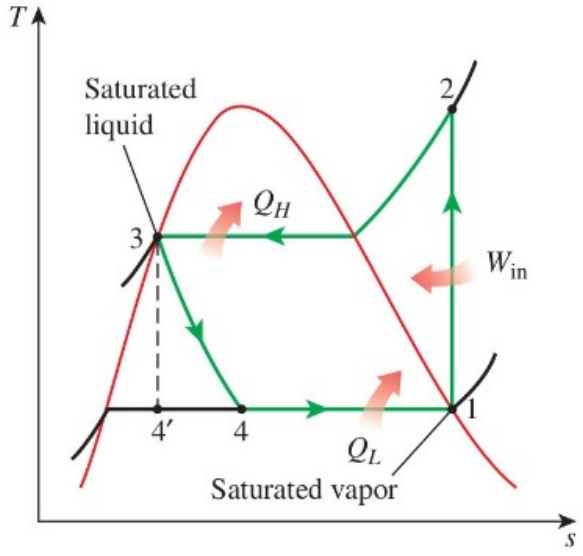

Figure 19: The assumed vapor compression system undergoes process (1,2,3 and 4) [11].

14. Analytical Calculations of Vapor Compression System

14.1 Mass Conservation Law

$$\dot{m}_{inlet} = \dot{m}_{outlet} = \dot{m} \tag{27}$$

14.2 Compression Work (W_c)

The inlet of the compressor is assumed to be saturated vapor which is to ensure all mixture constituents are vaporized. This assumption is critically important for the design of compressors in which it protects the compressor from two phase flow.

Compressor isentropic efficiency and work

$$\eta_c = \frac{W_{c,ideal}}{W_{c,real}} = \frac{(h_{2s} - h_1)}{(h_2 - h_1)} \tag{28}$$

Through the assumed isentropic efficacy (85%), the T_{2S} is the isentropic compression process and determined with the known parameters of s_g and P_f. Then, T_2 is determined assuming no heat loss at the compressor suction.

$$W_{c,real} = W_C = \dot{m}\,(h_2 - h_1) = \dot{m}\,(h_2 - h_g) \tag{29}$$

Where h_g is the saturated vapor inlet of the compressor

14.3 Condenser Energy (Heat) Transfer

The condenser is assumed to undergo isobaric process at the saturated liquid pressure.

$$Q_C = \dot{m}\,(h_3 - h_2) = \dot{m}\,(h_f - h_2) \tag{30}$$

Where h_f is the saturated liquid outlet of the condenser

14.4 Expansion Valve (Throttling Valve)

The expansion process is assumed to undergo isenthalpic process in which the saturated liquid enthalpy ($h_3 = h_f$) is equal to that of evaporator inlet.

$$(p_1 = p_g) \text{ and } (h_3 = h_4) \tag{31}$$

14.5 Evaporator Energy (Heat) Transfer

The evaporator is assumed to undergo isobaric process at the saturated vapor pressure.

$$Q_v = \dot{m}\,(h_1 - h_4) = \dot{m}\,(h_g - h_4) \tag{32}$$

Where h_g is the saturated vapor outlet of the evaporator

14.6 Coefficient of Performance of Cooling ($COP_{cooling}$)

$$COP_{cooling} = \frac{Q_V}{W_C} \tag{33}$$

14.7 Volumetric Cooling Capacity (Qc)

$$Qc = \frac{Q_V}{v_1} \tag{34}$$

15. Types of Mixtures in Evaporation and Condensation Processes

During isobaric process in the energy (heat) exchangers, mixtures can be categorized into three types of refrigerates mixtures.

15.1 Azeotropic Mixtures

Azeotropic mixtures evaporate and condensate with the same composition of vapor and liquid phases at isothermal and isobaric processes. A distinguishing factor of these mixtures is their zero temperature glide (TG) occurring between the saturated vapor and liquid and thus behave as pure refrigerants.

15.2 Zeotropic Mixtures (Non-Azeotropic).

Zeotropic mixtures are mixtures that have different mole fractions at the vapor phase and liquid phase when at equilibrium where it tends to change temperatures undergo an isobaric process, namely condensation and evaporation. This temperature difference occurs between the dew point and bubble point temperatures of which it exhibits a drop in the condensation process and an increase of temperature at the evaporation process. This variation is called temperature glide (TG). Composition shift is noticed as the mixture condensate or evaporate at equilibrium.

15.3 Near-Azeotropic Mixtures

Near-azeotropic mixture evaporate and condensate with small changes in their compositions of vapor and liquid phases that tends to exhibit comparatively small temperature glide (TG) at isobaric process in equilibrium conditions.

16. Result and Discussion

16.1 Working Fluids: Pure Refrigerants

- Propane (R-290)
- Propylene (R-1270)
- Dimethyl ether (R170)
- 50% Difluoromethane CH2F2 + 50% Pentafluoroethane CF3CHF2 (R-410)
- Difluoromethane (R32)
- 1,1,1,2-Tetrafluoroethane (R134a)
- 2,3,3,3-Tetrafluoropropene (R1234yf)
- 1,3,3,3-Tetrafluoropropene (R1234ze)

According to Figure 20, the R-410 and R-32 have the highest volumetric cooling capacity and shows acceptable (COP) of cooling. Therefore, they have been extensively used in the (AC) systems. The propane and propylene have better (COP) but lack the volumetric cooling capacity. similarly, the dimethyl ether shows the highest (COP) among all other refrigerants. The carbon dioxide has the highest cooling capacity and therefore blended with the hydrocarbons to compensate for the cooling capacity effect. The flammable refrigerants are in red and the high (GWP) refrigerants are in black.

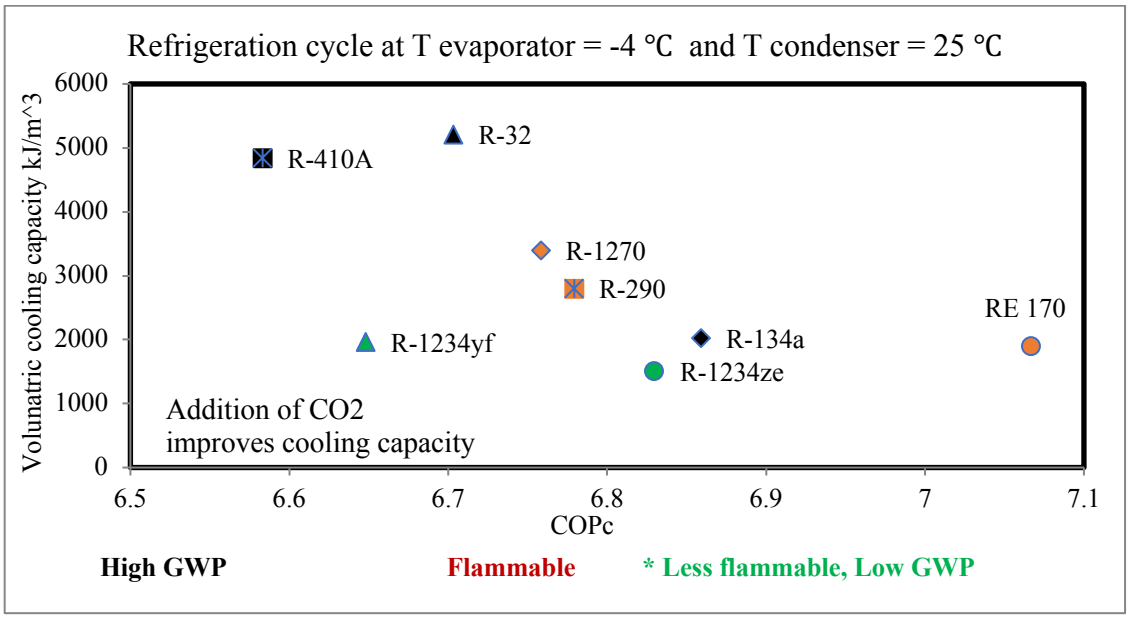

Figure 20: Pure refrigerants comparison with specific temperature condition.

16.2 Working Fluids: Mixture Refrigerants

16.2.1 System Coefficient of Performance (COP) and the Volumetric Cooling Capacity (Qc)

According to figure 21, the coefficient of performance (COP) as well as the volumetric cooling capacity (Qc) of n-butane refrigerant appears to be the lowest, it is thereafter be neglected due to its insufficient performance criteria of (COP) and (Qc) in this refrigeration system. The later analysis shows three hydrocarbons refrigerants, namely propane, propylene, and dimethyl ether. The solid lines represent the (COP) of the system. These refrigerants are blended with carbon dioxide (CO_2) and tested in different temperature conditions to simulate a typical case of refrigeration systems in room temperature climate as well as to simulate such a system in hot climate room temperature.

As seen in Figure 21, the volumetric cooling capacity of the mixtures improve upon the addition of the (CO_2). This demonstrates the fact that the (CO_2) has the highest volumetric cooling capacity among the chosen refrigerants and enhances the volumetric cooling capacity of the system when blended with these hydrocarbons. The propane + (CO_2) mixture as well as propylene + (CO_2) mixture illustrate similar performance and have higher volumetric cooling capacity than that of the dimethyl ether + (CO_2) mixture. The mixture of dimethyl ether + (CO_2) is lower at 90% mole fraction of (CO_2) in terms of volumetric cooling capacity because of its higher specific volume compared to the mixture of propane + (CO_2) and propylene + (CO_2).

According to Figure 22, the system (COP) is the highest obtained for room temperature of 25 ℃ at the condenser outlet. While Figure 23 shows the lowest (COP) for the case of room temperature. This difference is because of the work required by the compressor is lower at evaporator temperature of 4 ℃ than that of -15 ℃ . Therefore, the (COP) would be affected according to its definition. The idea is the same for room temperature of 45 ℃ at the condenser outlet. To illustrate, Figure 24 shows higher (COP) is obtained for all three mixtures while Figure 26 demonstrates a lower (COP) for all of these three mixtures and thus explained in detail in the following paragraphs.

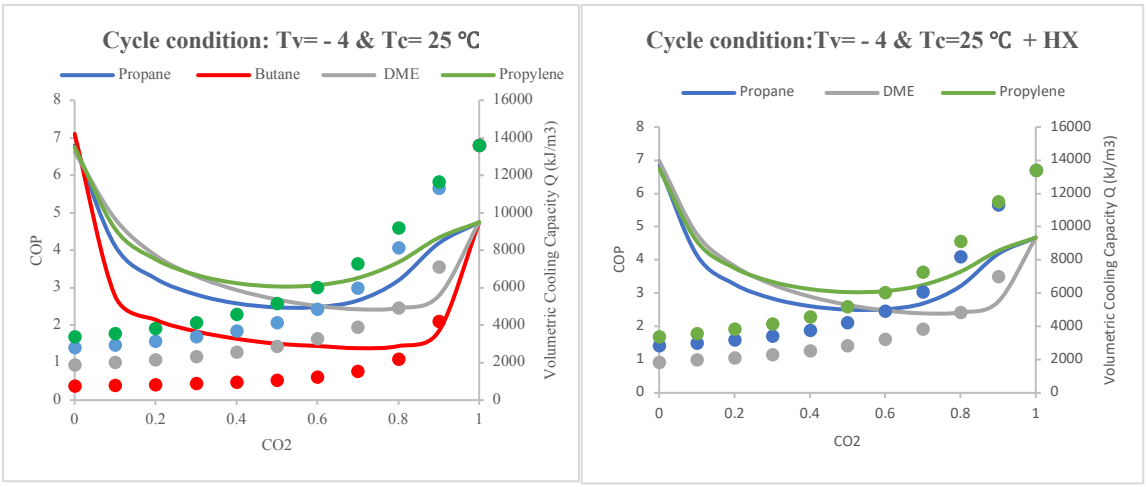

Figure 21: COP and volumetric cooling capacity for different refrigerants at initial selection.

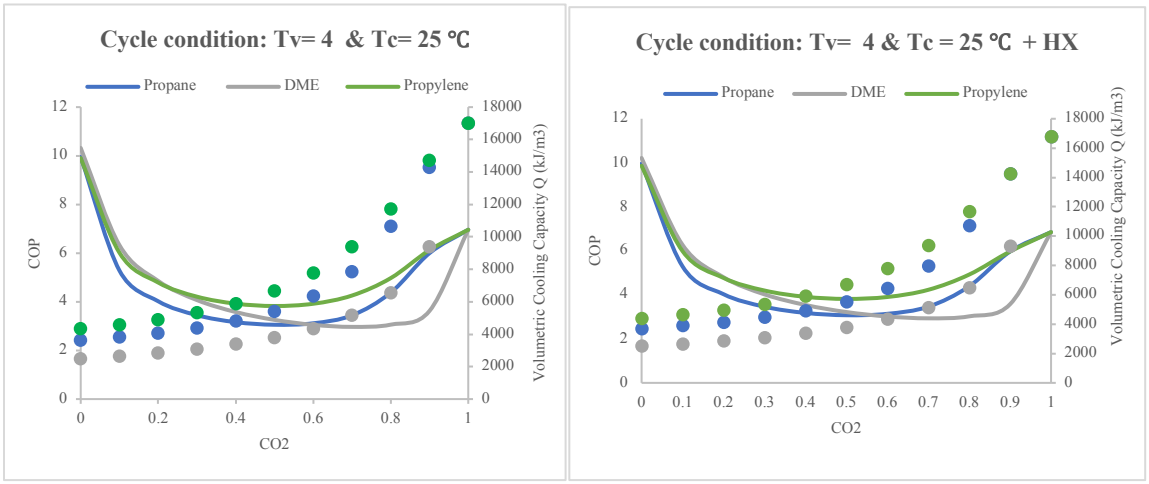

Figure 22: COP and volumetric cooling capacity vs ($\mathbf{CO_2}$) mole fraction of refrigerator side in room temperature.

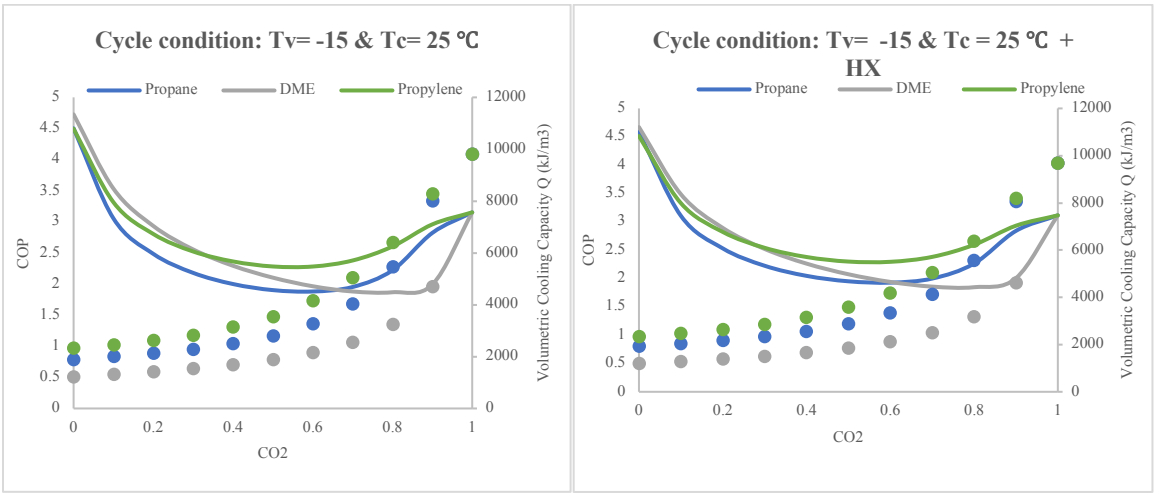

Figure 23: COP and volumetric cooling capacity vs ($\mathbf{CO_2}$) mole fraction of fridge side in room temperature.

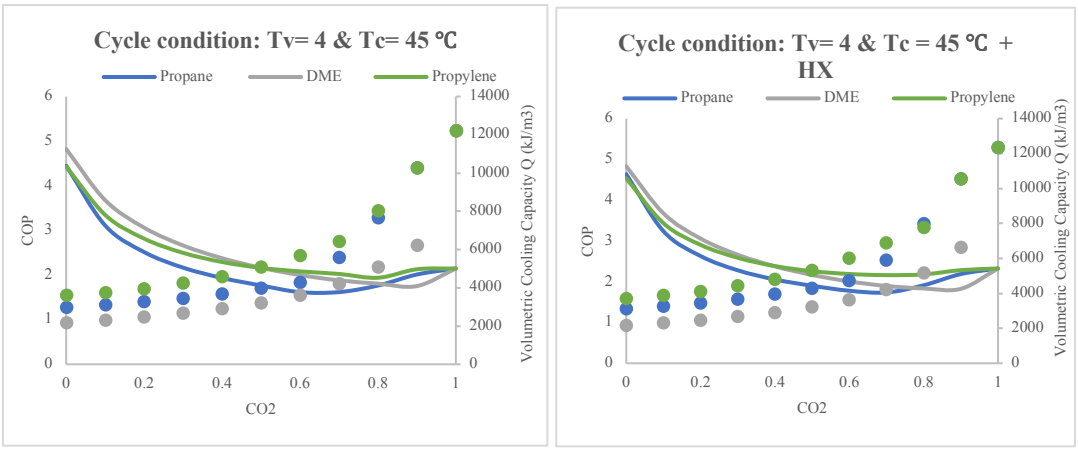

Figure 24: COP and volumetric cooling capacity with ($\mathbf{CO_2}$) mole fraction of refrigerator in hot climate room temperature.

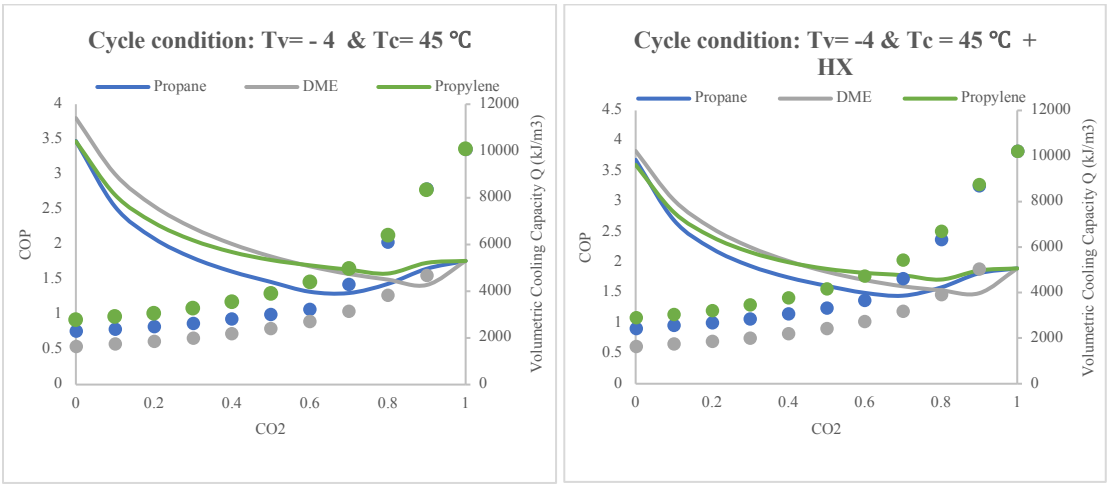

Figure 25: COP and volumetric cooling capacity with ($\mathbf{CO_2}$) mole fraction of fridge side in hot climate room temperature.

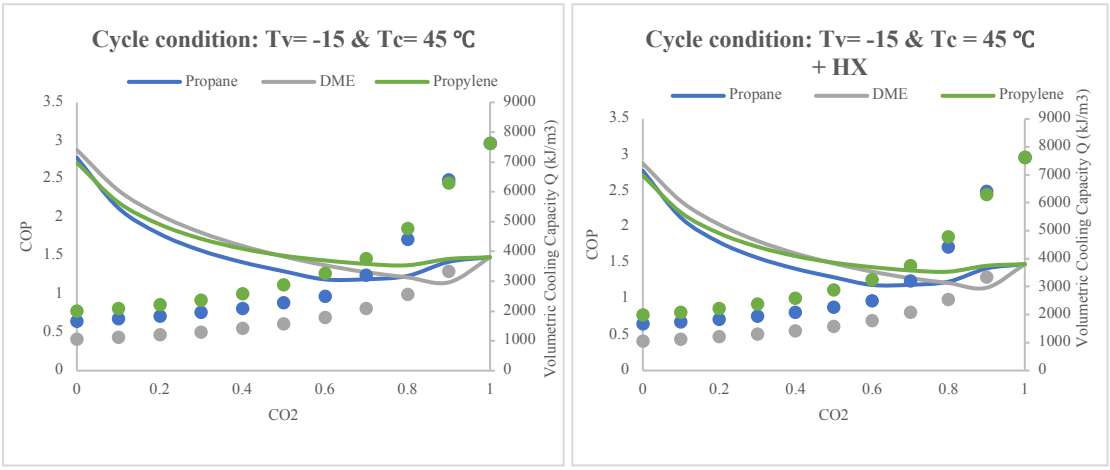

Figure 26: COP and volumetric cooling capacity with ($\mathbf{CO_2}$) mole fraction of fridge side in hot climate room temperature.

16.2.2 System COP and the Peak Pressure

Figure 27 illustrates the change of (COP) as a function of peak pressure with the addition of (CO_2). The solid lines represent the (COP) of the system. This helps identify the acceptable condenser exit pressure that corresponds to the (CO_2) mole fraction. By default, the higher the assumed temperature at the condenser exit, the higher the peak pressure. Additionally, The peak pressure increases when (CO_2) is added to the mixture; meaning that the inlet pressure (P1) is also increased. In the case of hot climate room temperature (45 ℃), approximately when the mixtures are at (≥ 70 % mole fraction) of (CO_2), then the critical temperatures of these three mixtures are higher than that of the operating temperatures which implies the system is operating on the transcritical cycle.

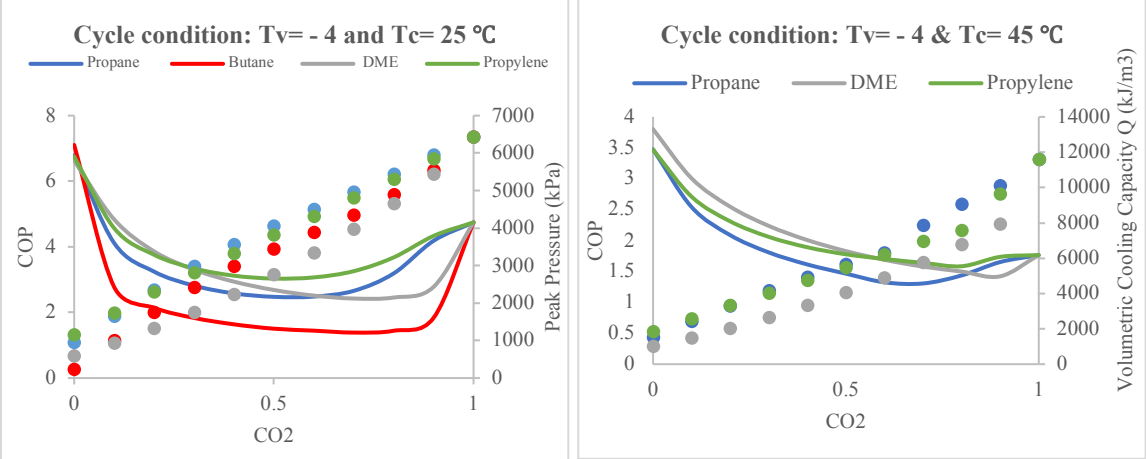

Figure 27: COP as a function of the Peak Pressure (P2).

16.2.3 System COP vs. Pressure Ratios

According to Figure 28, the pure hydrocarbons appear to enhance the system and provide the highest coefficient of performance (COP) because their pressure ratios are the lowest across the compressor's inlet and outlet. This pressure ratios increases with the addition of carbon dioxide (CO_2) mole fractions because carbon dioxide (CO_2) contains higher pressure based on Figure 30. This increase of pressure ratios drops above 50 % mole fraction of carbon dioxide (CO_2) due to the fact that the content of the carbon dioxide (CO_2) is higher than that of the hydrocarbons which increases the mixture inlet pressure (P1). The coefficient of performance (COP) is enhanced at (≥ 60 % mole fraction) of (CO_2) mixture as the pressure ratios continue to decrease.

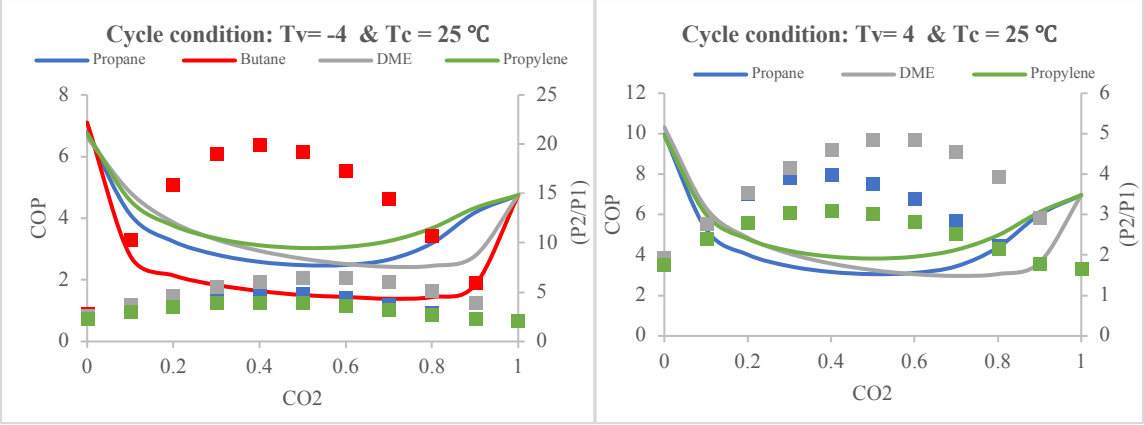

Figure 28: COP as a function of Pressure Ratios in the fridge (left) and refrigerator (right) sides at room temperature condition.

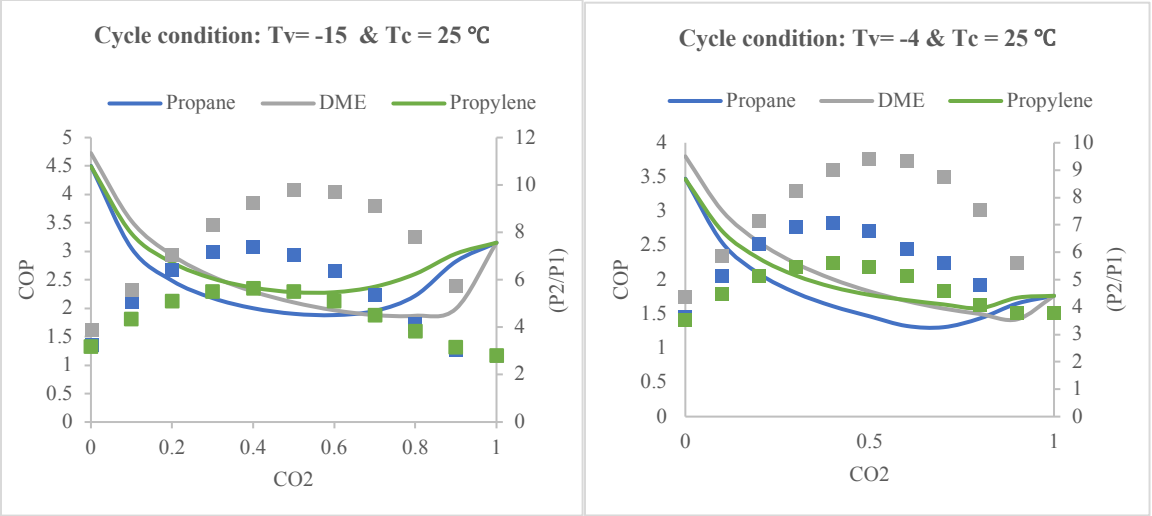

Figure 29: COP as a function of Pressure Ratios in the fridge side at room temperature condition.

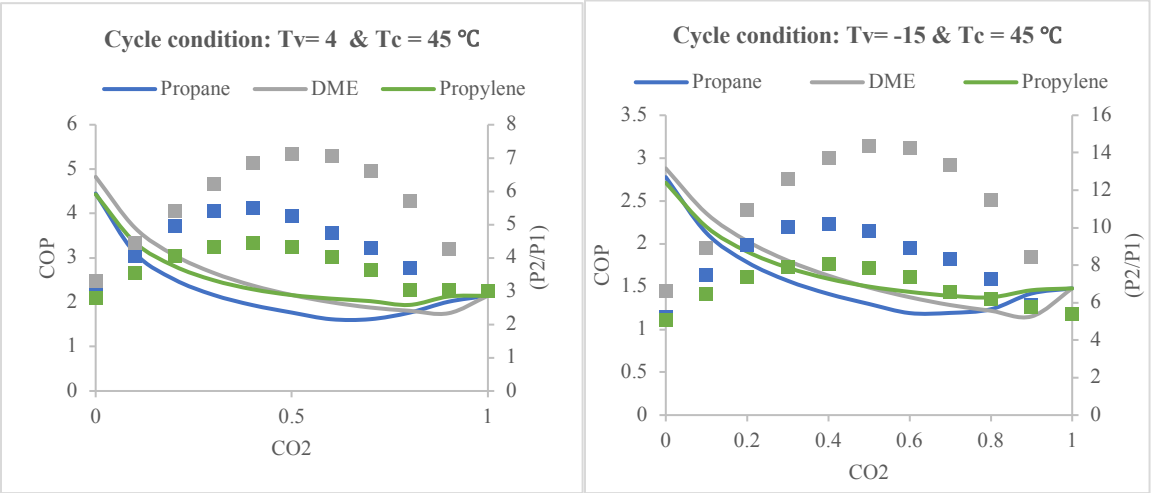

Figure 30: COP as a function of Pressure Ratios in the refrigerator (left) and fridge (right) sides at hot climate temperature condition.

16.2.4 Carbon Dioxide (CO_2) and the Compression Work

The (COP) as a function of compression work is illustrated on Figure 31 to show the difference of compression work required by the system in basic vapor compression system versus vapor compression system with an energy (heat) exchanger. The solid lines represent a compression work with no energy exchanger in the system. According to Figure 32, it can be seen that the compression work increases when the system has the energy exchanger between the condenser and the compressor. This increase of work is due to the fact that the inlet condition has changed from saturated vapor to superheated vapor region. Hence, the amount of work extracted from the superheated vapor region is higher than that work extracted from the saturated vapor region, namely for the basic compression system. This increase of work required by the compressor is demonstrated by chemical point of view. A study posted on Nature Communication has demonstrated this case for refrigerants with carbon components of (3) and higher such as propane and propylene. They concluded that these pure refrigerants may benefit from the energy exchanger depending on their heat capacity values. In this study of mixture refrigerants, the heat capacity plays a vital role in improving the (COP). For the case of dimethyl ether and (CO_2) mixture, the (COP) benefits from the addition of an energy exchanger at 80 % mole fraction of (CO_2) at exit temperature of 25 ℃. For more detail [18].

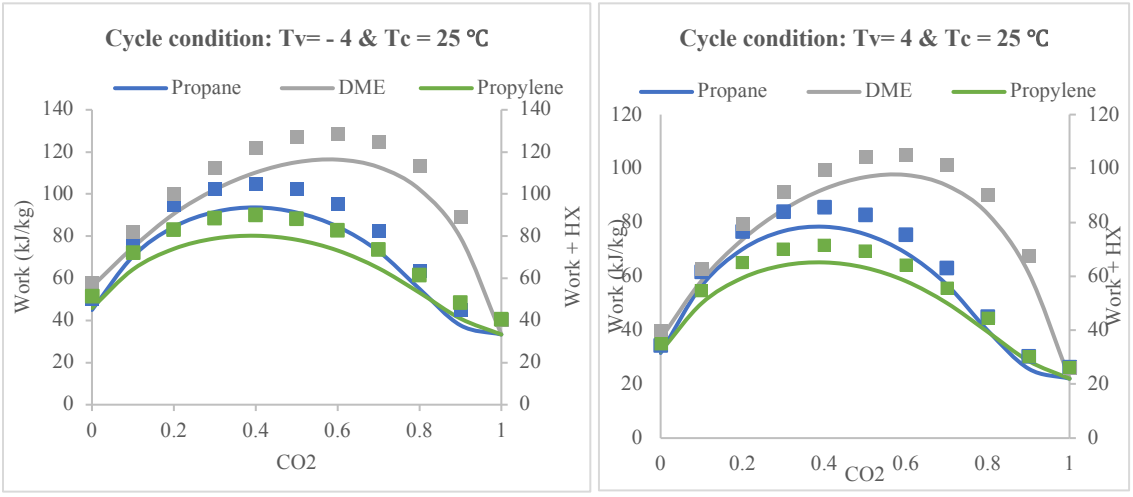

Figure 31: Compression work as a function of (CO_2) mole fractions at room temperature.

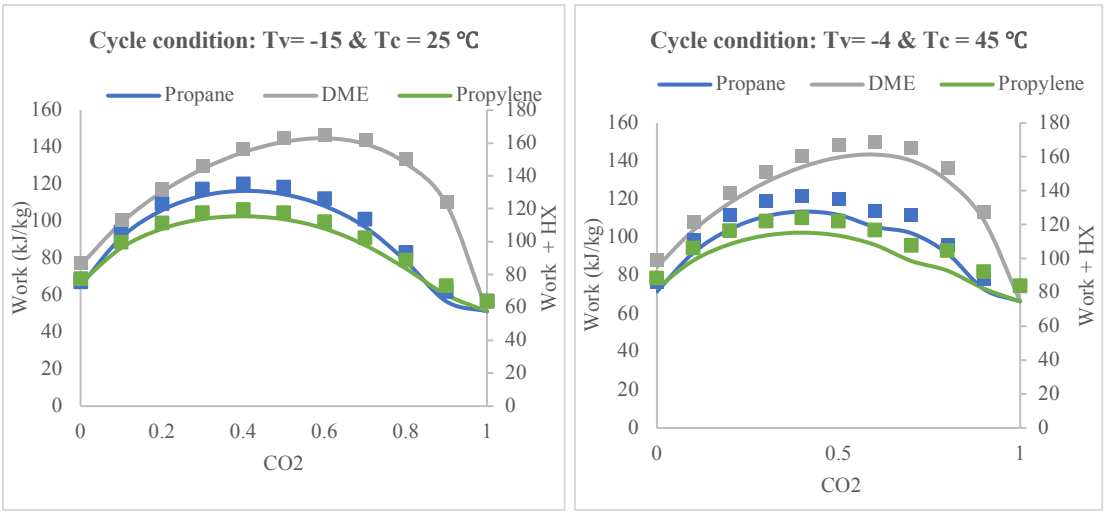

Figure 32: Compression work as a function of ($\mathbf{CO_2}$) mole fractions at room (left) and hot climate room temperatures (right).

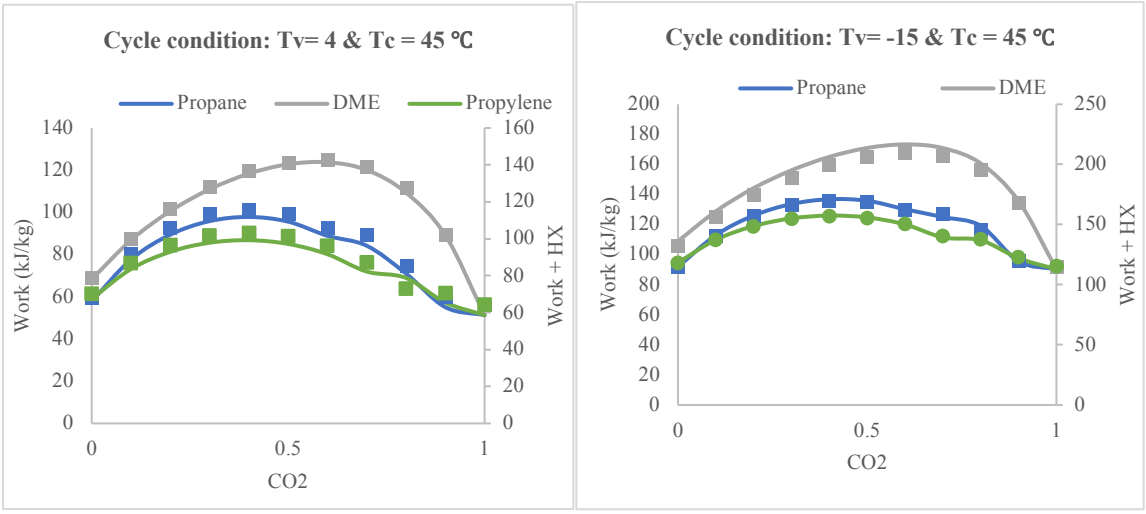

Figure 33: Compression work as a function of ($\mathbf{CO_2}$) mole fractions at hot climate room temperatures.

17. Summary and Conclusion

Alternative air conditioning (AC) refrigerants have been selected based on their thermophysical properties such as critical temperatures and pressures as well as their specific volumes as a function of carbon dioxide. These refrigerants have been studied on vapor compression system consisting of compressor, condenser, throttling valve, energy (heat) exchanger, and evaporator. The selected test conditions are for refrigeration system purposes such as evaporating temperatures of -15, -4, and 4 ℃. The outdoor temperatures were assumed at room temperatures of 25 and 45 ℃. According to the results, the propylene and propane demonstrated the highest coefficient of performance (COP) and volumetric cooling capacity (Qc) whereas the dimethyl ether showed improvements only at the (10% mole fraction) of carbon dioxide. The n-butane with carbon dioxide lowered the coefficient of performance (COP) and the volumetric cooling capacity (Qc) and therefore it should not be blended with carbon dioxide in refrigeration systems because of its high pressure ratios across the inlet and outlet of the compressor. The blend of propane, propylene, and dimethyl ether with carbon dioxide demonstrated sufficient coefficient of performance (COP) and volumetric cooling capacity (Qc) at mole fractions of 10 % and 90 % of carbon dioxide. These mixtures have been compared with the existing refrigerants such as R-410a and showed higher (COP) and (Qc) at the selected conditions. The flammability characteristic of those mixtures at mole fractions of 10% should be the cut-off point of decision of whether these refrigerants are safe and far away from a flame in its surroundings. By comparison to the current refrigerant (R-410a), the blends of those hydrocarbons with carbon dioxide at mole fraction of 90% are also better in terms of (COP) and (Qc). The operating pressure of this 90% mole fraction needs highly-temperature resistive materials that operate at the supercritical region to prevent damage due to this high pressure.

18. REFERENCES

[1]. Hofmann, D. J., J. H. Butler, E. J. Dlugokencky, J. W. Elkins, K. Masarie, S. A. Montzka, and P. Tans, (2006a), The role of carbon dioxide in climate forcing from 1979 - 2004: Introduction of the Annual Greenhouse Gas Index, Tellus B, 58B, 614-619.

[2]. WMO (World Meteorological Organization), Scientific Assessment of Ozone Depletion: 2010, Global Ozone Research and Monitoring Project–Report No. 52, 516 pp., Geneva, Switzerland, 2011.

[3]. Montreal Protocol on Substances that Deplete the Ozone Layer: Report of the Halon Fire Extinguishing Agents Technical Options Committee: UNEP December 1994.

[4]. NIST Standard Reference Database 23, "NIST Reference Fluid Thermodynamic and Transport Properties—REFPROP, Version 9.1," (Standard Reference Data Program, 2013).

[5]. NIST Reference Fluid Thermodynamic and Transport Properties—REFPROP Version 9.1 User's Guide. https://www.nist.gov/sites/default/files/documents/srd/REFPROP9.PDF.

[6]. B. A. Younglove and J. F. Ely, "Thermophysical Properties of Fluids. II. Methane, Ethane, Propane, Isobutane, and Normal Butane," journal of Physical and Chemical Reference Data 16, 577 (1987).

[7]. Lemmon, E.W., McLinden, M.O., Wagner, W. "Thermodynamic Properties of Propane. III. Reference Equation of State for Temperatures from the Melting Line to 650 K and Pressures up to 1000 MPa," J. Chem. Eng. Data, 54:3141-3180, 2009.

[8]. Perkins, R. A.; Sanchez Ochoa, J. C.; Magee, J. W. J. Chem. Eng. Data 2009, in press.

[9]. Setzmann, U.; Wagner, W. J. Phys. Chem. Ref. Data 1991, 20, 1061–1155.

[10]. Span, R. and Wagner, W.,"A New Equation of State for Carbon Dioxide Covering the Fluid Region from the Triple-Point Temperature to 1100 K at Pressures up to 800 MPa," J. Phys. Chem. Ref. Data, 25(6):1509-1596, 1996.

[11]. Fundamentals of Engineering Thermodynamics, 8th Edition, Michael J. MoranHoward N. ShapiroDaisie D. BoettnerMargaret B. Bailey May 5, 2014, Wiley Global Education (1987).

[12]. Kunz, O; Kalmuck, R; Wagner, W; Marschke, M; 'The GERG-2004 Wide-Range Equation of State for Natural Gases and Other Mixtures' GERG TECHNICAL MONOGRAPH 15 (2007).

[13]. Lemmon, E. W., Roth, R. T; 'A Helmholtz energy equation of state for calculating the thermodynamic properties of fluid mixtures' Fluid phase Equilibria, 165 1999 1–21.

[14]. Gyftopoulos, E. and Beretta, G.P. (2005) Thermodynamics: Foundations and Applications. Dover Publications, New York.

[15]. Wu, J., Zhou, Y., and Lemmon, E.W. "An equation of state for the thermodynamic properties of dimethyl ether," J. Phys. Chem. Ref. Data, 40(023104):1-16, 2011.

[16]. Buecker, D. and Wagner, W.,"Reference Equations of State for the Thermodynamic Properties of Fluid Phase n-Butane and Isobutane,"J. Phys. Chem. Ref. Data, 35(2):929-1019, 2006.

[17]. Richter, M., McLinden, M.O., and Lemmon, E.W."Thermodynamic Properties of 2,3,3,3-Tetrafluoroprop-1-ene (R1234yf): Vapor Pressure and p-rho-T Measurements and an Equation of State," J. Chem. Eng. Data, 56(7):3254-3264, 2011.

[18]. McLinden, M. O. et al., "Limited options for low-global-warming potential refrigerants," Nature Communications., 8, 14476 doi: 10.1038/ncomms14476, (2017).

[19]. Kunz, O., Klimeck, R., Wagner, W., Jaeschke, M. The GERG-2004 Wide-Range Equation of State for Natural Gases and Other Mixtures. GERG Technical Monograph 15. Fortschr.-Ber. VDI, VDI-Verlag, Düsseldorf, 2007.

[20]. Kunz, O. and Wagner, W. The GERG-2008 Wide-Range Equation of State for Natural Gases and Other Mixtures: An Expansion of GERG-2004. J. Chem. Eng. Data, 57(11):3032-3091, 2012.

[21]. W.E. Acree, Jr., J.S. Chickos, "Phase Transition Enthalpy Measurements of Organic and Organometallic Compounds" in NIST Chemistry WebBook, NIST Standard Reference Database Number 69,

Eds. P.J. Linstrom and W.G. Mallard, National Institute of Standards and Technology, Gaithersburg MD, 20899.

[22]. Guus J. M. Velders, David W. Fahey, John S. Daniel, Mack McFarland, Stephen O. Andersen. The large contribution of projected HFC emissions to future climate forcing Proceedings of the National Academy of Sciences Jul 2009.

[23]. Rajapaksha, Leelananda, "Influence of special attributes of zeotropic refrigerant mixtures on design and operation of vapor compression refrigeration and heat pump systems," Energy Convers. Management., 48 (2), pp. 539-545, (2007).

19. APPENDIX

Appendix A: The Real Gas Contribution Terms of the Helmholtz Free Energy.

k	N_k	t_k	d_k	l_k	η_k	β_k	γ_k	ε_k
1	0.042910051	1.00	4					
2	1.7313671	0.33	1					
3	-2.4516524	0.80	1					
4	0.34157466	0.43	2					
5	-0.46047898	0.90	2					
6	-0.66847295	2.46	1	1				
7	0.20889705	2.09	3	1				
8	0.19421381	0.88	6	1				
9	-0.22917851	1.09	6	1				
10	-0.60405866	3.25	2	2				
11	0.066680654	4.62	3	2				
12	0.017534618	0.76	1	-	0.963	2.33	0.684	1.283
13	0.33874242	2.50	1	-	1.977	3.47	0.829	0.6936
14	0.22228777	2.75	1	-	1.917	3.15	1.419	0.788
15	-0.23219062	3.05	2	-	2.307	3.19	0.817	0.473
16	-0.092206940	2.55	2	-	2.546	0.92	1.500	0.8577
17	-0.47575718	8.40	4	-	-3.28	18.8	1.426	0.271
18	-0.017486824	6.75	1	-	14.6	547.8	1.093	0.948

Appendix B: The modified benedict web equation of state is as follows:

$$P=\rho RT+\rho^2[G(1)T+G(2)T^{1/2}+G(3)+G(4)/T+G(5)/T^2]+\rho^3[G(6)T+G(7)+G(8)/T+G(9)/T^2]$$
$$+\rho^4[G(10)T+G(11)+G(12)/T]+\rho^5[G(13)]+\rho^6[G(14)/T+G(15)/T^2]+\rho^7[G(16)/T]$$
$$+\rho^8[G(17)/T+G(18)/T^2]+\rho^9[G(19)/T^2]+\rho^3[G(20)/T^2+G(21)/T^3]\exp(\gamma\rho^2)$$
$$+\rho^5[G(22)/T^2+G(23)/T^4]\exp(\gamma\rho^2)+\rho^7[G(24)/T^2+G(25)/T^3]\exp(\gamma\rho^2)$$
$$+\rho^9[G(26)/T^2+G(27)/T^4]\exp(\gamma\rho^2)+\rho^{11}[G(28)/T^2+G(29)/T^3]\exp(\gamma\rho^2)$$
$$+\rho^{13}[G(30)/T^2+G(31)/T^3+G(32)/T^4]\exp(\gamma\rho^2).$$

Where G (1) to G (32) are coefficients in form of (10^{-3}) and found in appendix J. for propane, for more details [7]. These coefficients don't do any fitting terms that are used to calculate accurate thermodynamics properties. Gamma is not fitted terms and is equal to ($\gamma = 1/\rho_c^2$).

Appendix C: pressure of saturated vapor as function of carbon dioxide.

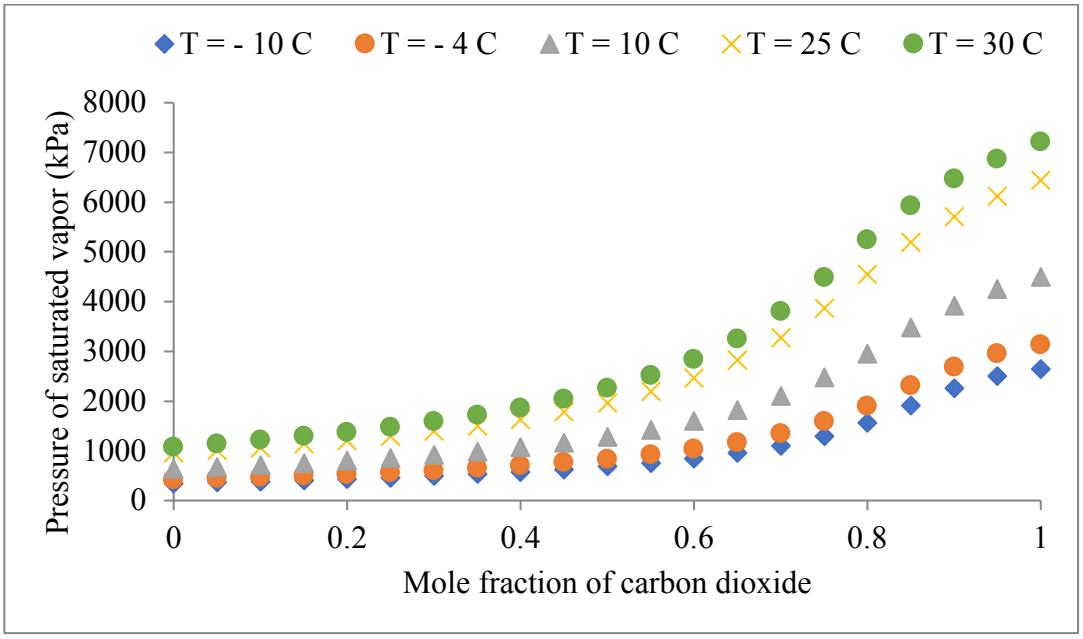

Figure C1: Pg variations with mole fraction of carbon dioxide.

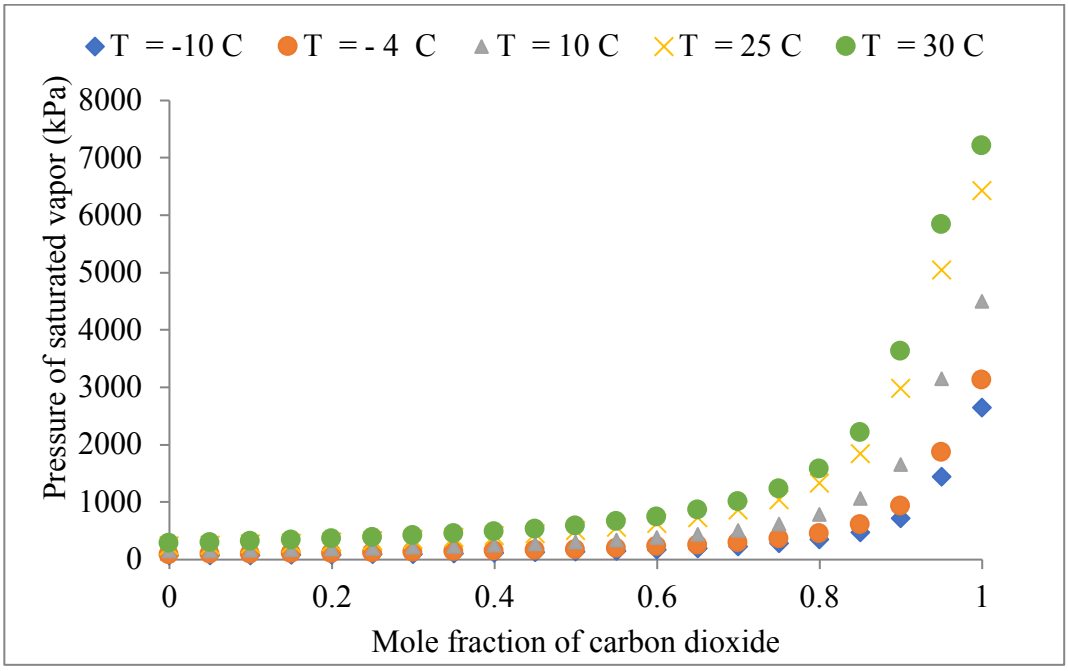

Figure C2: Pg variations with mole fraction of carbon dioxide.

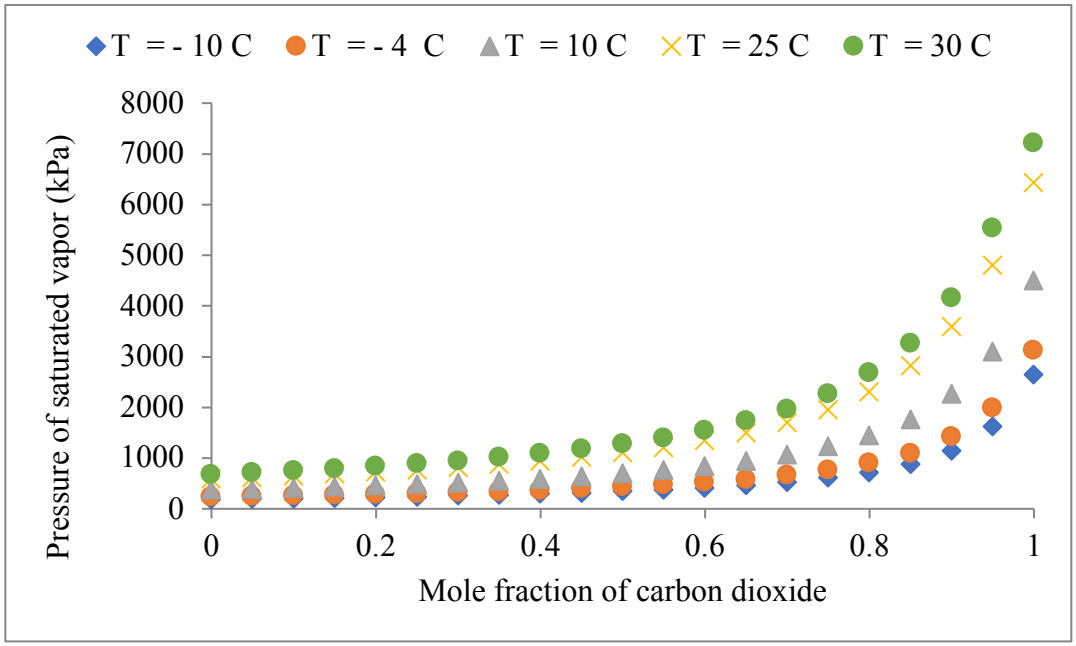

Figure C3: *Pg* variations with mole fraction of carbon dioxide.

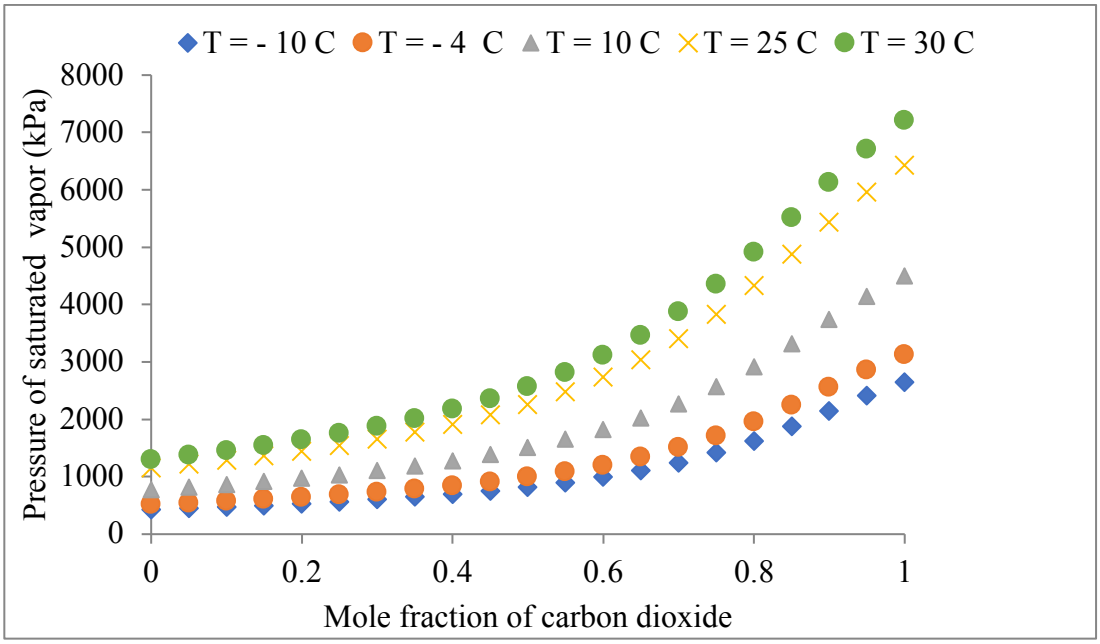

Figure C4**:** *Pg* variations with mole fraction of carbon dioxide.

Appendix D: Mixture as a function of carbon dioxide at constant temperatures and pressures

n-Butane + Carbon Dioxide at constant temperatures

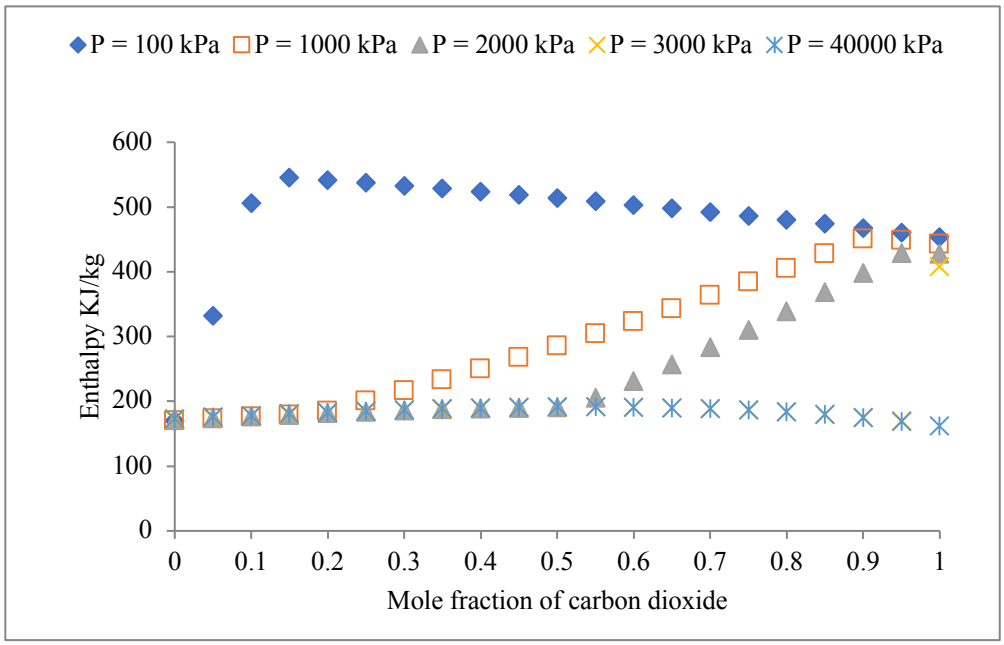

Figure D1: Enthalpy as function of carbon dioxide at constant T = - 4 °C.

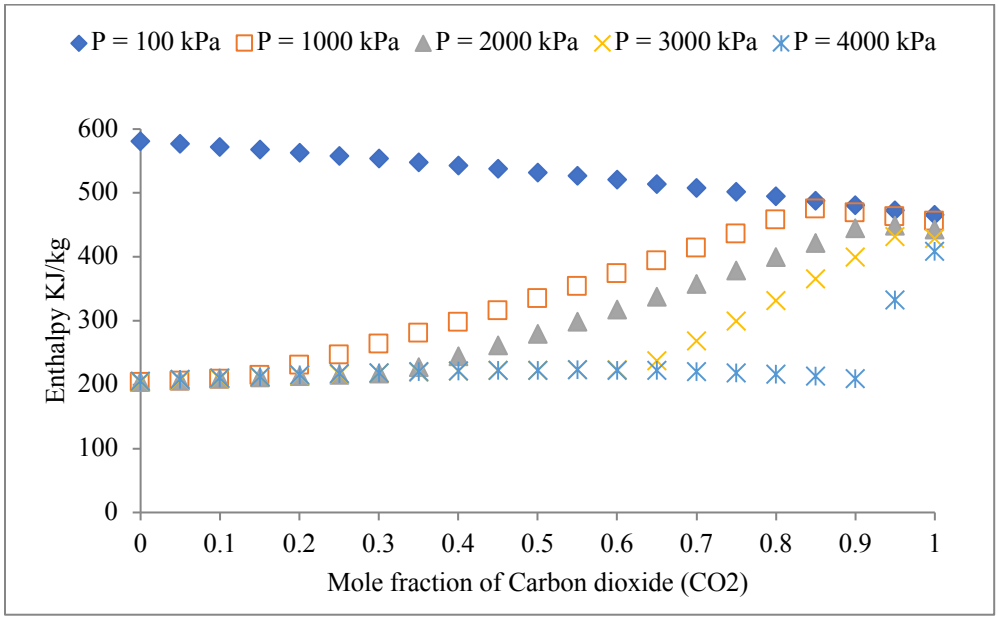

Figure D2: Enthalpy as function of carbon dioxide at constant T = 10 °C

Dimethyl ether + Carbon Dioxide at constant temperatures

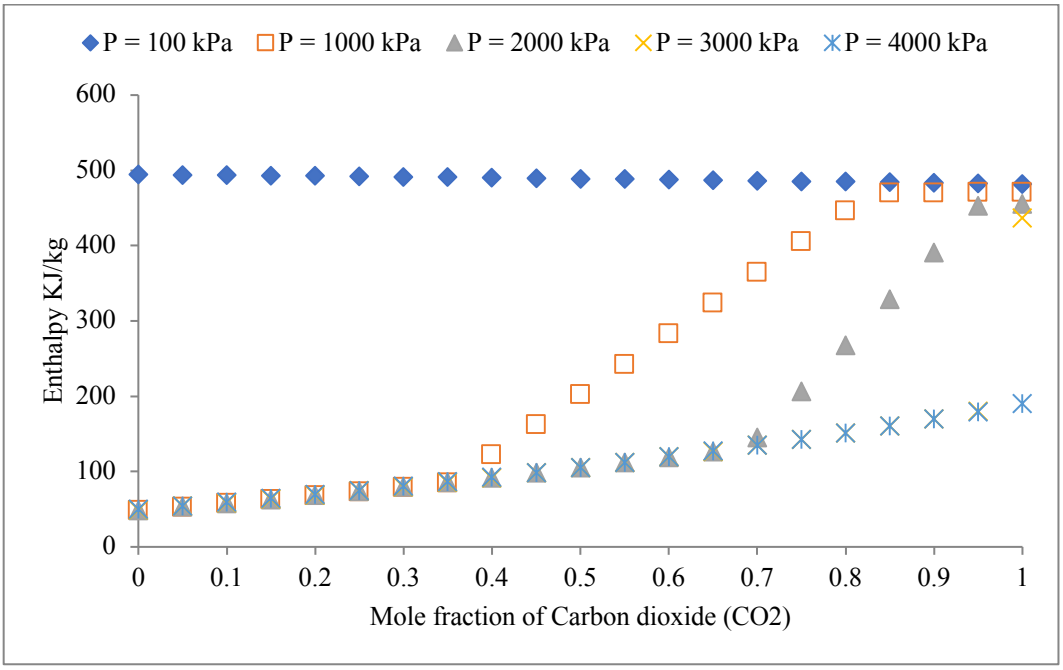

Figure D3: Enthalpy as function of carbon dioxide at constant T = - 4 °C

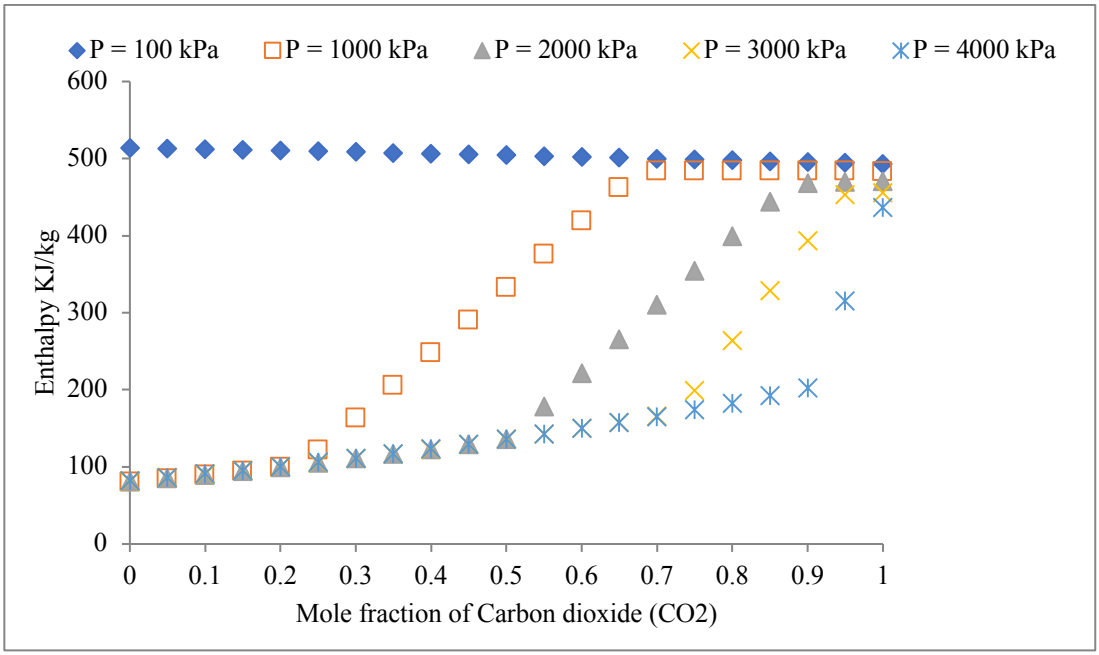

Figure D4: Enthalpy as function of carbon dioxide at constant T = 10 °C.

Propylene + Carbon Dioxide at constant temperatures

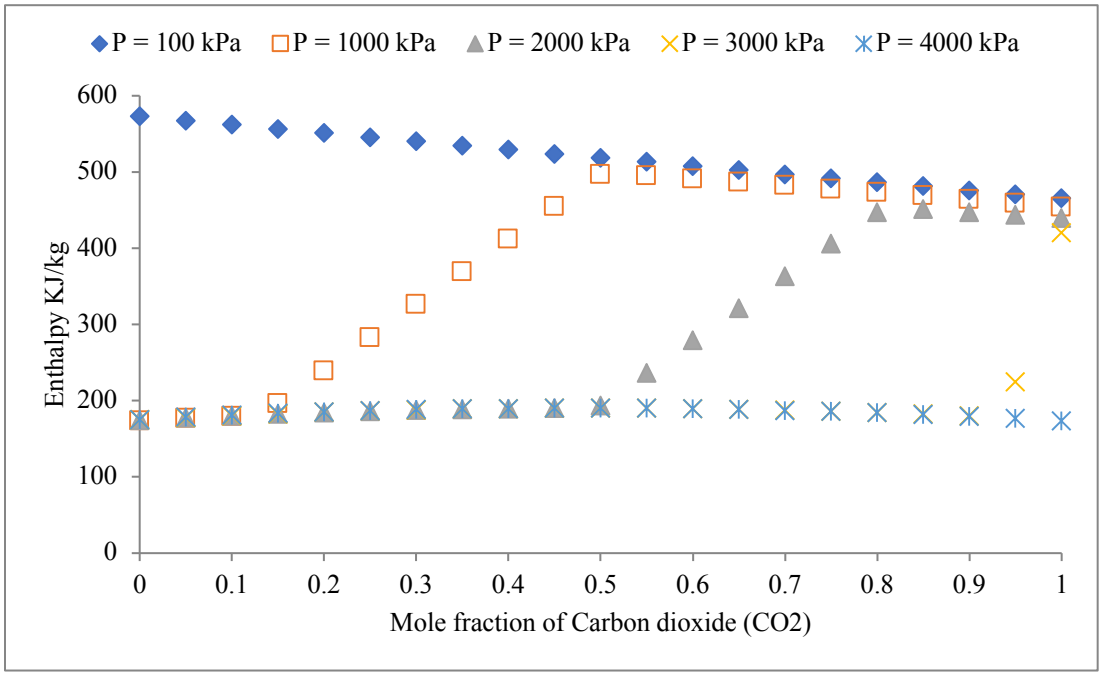

Figure D5: Enthalpy as function of carbon dioxide at constant T = - 4 ℃.

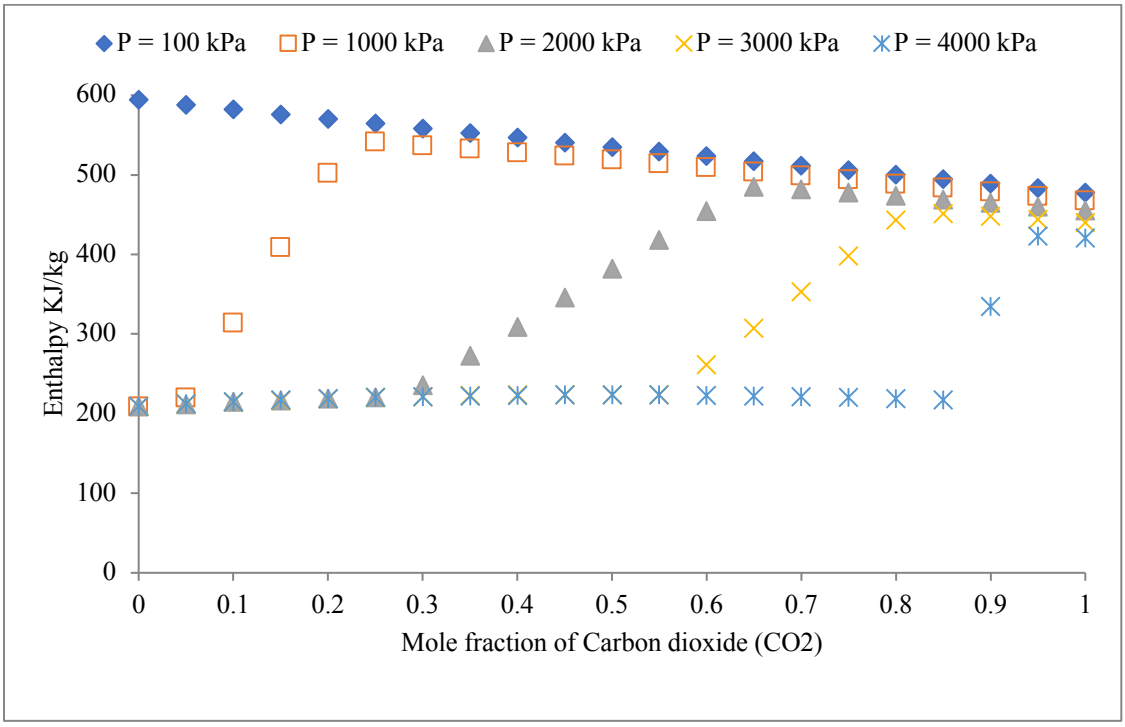

Figure D6: Enthalpy as function of carbon dioxide at constant T = 10 ℃.